



Title	Evaluation of inflammatory response during the wound healing process in caries-induced pulpitis model
Author(s)	黄, 海玲
Citation	大阪大学, 2022, 博士論文
Version Type	VoR
URL	<a href="https://doi.org/10.18910/87965">https://doi.org/10.18910/87965</a>
rights	
Note	

*The University of Osaka Institutional Knowledge Archive : OUKA*

<https://ir.library.osaka-u.ac.jp/>

The University of Osaka

**Evaluation of inflammatory response during the  
wound healing process in caries-induced pulpitis  
model**

**Huang Hailing**

**Ph.D. Dissertation**

Osaka University Graduate School of Dentistry

Course for Oral Science

Department of Restorative Dentistry and Endodontology

Supervisor: Professor Mikako Hayashi

## ACKNOWLEDGMENT

I would like to acknowledge and give my sincere appreciation to my supervisor, Professor Hayashi Mikako, the head of Department of Restorative Dentistry and Endodontology, Osaka University Graduate School of Dentistry. Her guidance and support carried me through all the stages of my project.

I would also like to extend many thanks to Associate Professor Takahashi Yusuke for providing me valuable advice and a lot of supports in my research work. I will not achieve all the progress without his guidance and support.

I would like to thank my group members Dr. Okamoto Motoki, Dr. Watanabe Masakatsu, Matsumoto Sayako, and Moriyama, Kiichi for their kind supports and assistance. I truly grateful to all the teachers and members in our department as well. I have embraced a lot of beautiful memories with them in my staying at this department. All of these good moments became treasures in my life.

I'd like to give special thanks to my family as a whole for their continuous support and understanding of my decision to continue studying.

In the end, I appreciate TERAYAMA FOUNDATION, Japanese Ministry of Education, Culture, Sports, Science and Technology for their financial assistance at third year and fourth year of my PhD.

# INDEX

## **Chapter 1 - Introduction**

<b>1.1. General introduction</b>	1
<b>1.2. Objectives</b>	5

## **Chapter 2 - Establishment of caries-induced pulpitis model**

<b>2.1. Materials and Methods</b>	
2.1.1. Caries induction protocols	7
2.1.2. Characterization of caries progression	9
2.1.3. Histopathological evaluation of inflamed pulp	9
<b>2.2. Results</b>	12
<b>2.3. Discussion</b>	15

## **Chapter 3 - Tertiary dentin formation in caries-induced pulpitis model**

<b>3.1. Materials and Methods</b>	
3.1.1. Direct pulp capping procedure	19

3.1.2. Micro-CT analysis and histological analysis	20
3.2. Results	20
3.3. Discussion	21
<b>Chapter 4 - Assessment of inflammatory changes during wound healing process of reversible pulpitis after pulp capping with ProRoot MTA</b>	
4.1. Materials and Methods	
4.1.1. Animal experiments and histological analysis	25
4.1.2. Quantification of relative numbers of positive cells in immunohistochemistry	25
4.1.3. Statistical analysis	26
4.2. Results	26
4.3. Discussion	28
<b>Chapter 5 - Conclusion</b>	32
<b>Chapter 6 - References</b>	33
<b>Chapter 7 - Figures and tables</b>	43

## **Abbreviations**

IL-6: Interleukin-6

IFN- $\gamma$ : Interferon-gamma

Micro-CT: Micro-computed tomography

MSB: Mitis salivarius-bacitracin

MSCs: Mesenchymal stem cells

PCNA: Proliferating cell nuclear antigen

PRRs: Pathogen pattern recognition receptors

PBS: Phosphate buffered saline

TNF-alpha: Tumor necrosis factor-alpha

TGF-beta: Transforming growth factor-beta

TLR2: Toll like receptor 2

# Chapter 1

## Introduction

### 1.1. General Introduction

Dental pulp tissue, positioned on the most inner side of tooth structure, consists of the soft connective tissue, nerve fibers, and blood vessels, including multiple types of cells that possess the specialized function of maintaining the biological and physiological vitality of the tooth [1]. Dental pulp is often exposed due to several damaging processes, including caries, trauma, or iatrogenic reasons, such as tooth preparation, which can lead to inflammation of the dental pulp (pulpitis) [2]. Direct pulp capping is a vital pulp therapy that promotes the self-healing capacity of pulp tissue using capping materials, such as calcium hydroxide or calcium silicate cement, over the exposed pulp [2-4]. This therapy is expected to restore the injured pulp back to homeostasis and induce complete tertiary dentin formation in the exposed site to produce a physical barrier between external stimuli and the pulp [4]. The success rate of vital pulp therapy depends on the accurate diagnosis of pulpal status, which can allow the repair process to occur. It has been reported that when the pulp is exposed during caries removal, which indicates that the residual infectious substrate could remain in the pulp, the success rate of direct pulp capping is relatively low because of difficulties in controlling the infection and inflammation of the pulp [5,6]. Therefore, in order to improve clinical outcomes, there is a need to understand the comprehensive correlation between inflammation and wound healing in the peripheral area of the pulp.

To date, the clinical diagnosis of reversible and irreversible pulpitis has been based on the common presenting complaints by patients, including pain (i.e. type, intensity, stimulus, and referred pain), as well as clinical findings using thermal or electronic tests or radiographic examination of the tooth and periapical tissue [7]. However, many clinical studies have illustrated that there is little correlation between clinical symptoms and the severity of inflammation in the dental pulp [8-10], and this inconsistency may be a reason for the lower success rate of vital pulp therapy. Many patients seek emergency dental treatment because of intense pain caused by acute pulpitis, which may be reversible or irreversible. One clinical study reported that almost 40% of irreversible pulpitis cases were asymptomatic [11]. Therefore, the chief complaint may not be a reliable factor in determining whether dental pulp damage is reversible. While histological evaluation is considered to be the gold standard for determining the inflammatory status of the pulp tissue [10,12], but this method cannot be performed in clinical situations. Prospective animal studies and human case reports have defined reversible or irreversible pulpitis by the presence of bacteria or bacterial by-products in peripheral dental pulp, the persistence of inflammatory conditions (predominance of inflammatory cells), or necrotic tissue [8,13]. However, little is known about the healing capacity of pulp under such inflammatory conditions.

Multiple immune cell types play a role in protecting the dental pulp against foreign bodies when pulp exposure occurs due to damage to the tooth structure. According to one review paper published in 2007, the innate effector immune cells in the dental pulp are neutrophils, dendritic cells, macrophages, and lymphocytes [14]. Among these, macrophages and dendritic cells are considered to exist since tooth development,



with macrophages being the only immune cell type that is involved in both inflammation and healing [14, 18]. Wound healing is a highly programmed process that is involved in a variety of cellular and molecular events. It includes hemostasis, inflammation, proliferation, and remodeling phases. In particular, the transition from the inflammatory phase to the proliferative phase plays a pivotal role in determining wound healing outcomes [15,16]. Macrophages can be found in all tissues and show great functional diversity by controlling the balance of their polarization to different phenotypes to facilitate the inflammatory-proliferative phase transition. Previous studies have demonstrated that macrophages can polarize into two subtypes during wound healing. M1 macrophages dominate during the inflammatory phase and mediate host defense against pathogens by releasing pro-inflammatory cytokines, such as interleukin (IL)-6 and tumor necrosis factor (TNF)-alpha. M2 macrophages have anti-inflammatory roles that contribute to tissue repair by expressing high levels of mannose receptor, IL-10, transforming growth factor (TGF)-beta, etc. [17-19]. The balance between M1 and M2 macrophages is considered to play an important role in regulating the wound healing phases [20,21]. Numerous studies have found that M2 macrophages may play pivotal roles in the maintenance of homeostasis and tissue repair after injury [18-22]. Furthermore, it has been reported that the population of macrophages is predominant in inflamed human pulp tissue, whose diagnosis is irreversible pulpitis [23-25]. Considering that macrophages can be involved not only in the inflammatory process but also in the later healing process, we assume that evaluating the polarization of macrophages in inflamed pulp could provide clues for identifying the boundary line between reversible pulpitis and irreversible pulpitis.

Rodent animal models for pulp capping have been widely used in dental research because of the similarity of their tooth structure and cellular processes with those of humans [26]. Hence, the essential biological responses of the pulp tissue and the interaction during the different stages of wound healing in rat molar teeth are comparable to those of other mammals. However, most pulp capping studies using rodents have been conducted on non-infected sound teeth, which are not true mimics of the clinical situation. Therefore, pulpal cellular and molecular processes of inflammatory reactions under caries invasion have not been considered in the conventional sound rat pulp capping model [27]. In addition, the conventional methods in investigating pulp inflammation using rodent animal models are to create an artificial pulp exposure by cavity preparation followed by the addition of bacterial components or left it open to induce inflammation [28]. The methods for the assessment of inflammation vary among different reports and include histological methods, flow cytometry analysis, and the evaluation of the gene and protein levels using polymerase chain reaction (PCR) [29-31]. Although the pulpal inflammation model using these assessments could be used to evaluate the immune reaction in the exposed pulp, it has limitations when investigating the initial pulpal inflammation caused by carious stimuli. In our previous study, we reported that some intrinsic proteinases released from the organic dentin matrix during caries progression could affect the pulpal wound healing process [32, 33]. Therefore, existing animal models may not be able to accurately evaluate the inflammatory transition after vital pulp therapy. Furthermore, little is known about how caries-induced inflammation can affect the outcome of pulpal wound healing. Thus, there is a need to develop a new pulp capping animal model involving caries-induced inflammation to mimic the

clinical situation.

Rodent caries models have long been used to investigate human oral diseases, producing much of our current understanding of caries pathology, treatment, and prevention [34-36]. However, due to a lack of research on caries lesions with pulp status, few studies have used a caries model to evaluate the outcome of vital pulp therapy (e.g., pulp capping). Hence, the challenge of using a rodent caries model for the evaluation of vital pulp therapy is to understand the pulp inflammatory status under different caries progression before treatment. Recently, with the development of digital image visualization techniques, X-ray computed micro-tomography (micro-CT) has become widely used as a sequential measurement in the evaluation of caries progression and various other aspects of the tooth [37,38], allowing us to observe caries progression in a non-destructive manner. To address the lack of research evaluating the pulp status in the caries model, in the present study, we evaluated inflammatory status under different stages of caries progression and produced a criterion for rat caries-induced reversible/irreversible pulpitis model for direct pulp capping.

## **1.2. Objectives**

The purpose of this study was to establish a rat caries-induced pulpitis model and to evaluate the inflammatory changes during the wound healing process after pulp capping in a reversible pulpitis model induced by caries.

In Chapters 2, 3, and 4, we first present our investigation of the inflammatory status of the pulp under different carious progression. Afterward, direct pulp capping was performed in a reversible and irreversible pulpitis model to elucidate the treatment outcomes under different inflammatory conditions. Finally, inflammatory changes in reversible pulpitis during the wound healing process were investigated.

## Chapter 2

### Establishment of caries-induced pulpitis model

#### 2.1. Materials and Methods

##### 2.1.1. Caries induction protocols

###### a) Animals

All experimental procedures using animals were approved by the Institutional Animal Care and Use Committee of Osaka University Graduate School of Dentistry (no. R-01-017-0). Dental caries was induced using a previously described method [39]. Fourteen-day-old male Sprague-Dawley rats (n = 30) were obtained from three dams and housed in plastic cages on corncob bedding. The animals were fed with tetracycline (4 g/kg) (FUJIFILM Wako Pure Chemical Corporation, Osaka, Japan) containing powdered food and water containing penicillin G potassium (4000 U/mL) (Meiji Seika Pharma Co., Ltd, Osaka, Japan) for three days to remove non-specific pathogens before the caries induction procedure.

###### b) Cariogenic bacterial culture and inoculation preparation

The streptomycin-resistant strain from *Streptococcus mutans* MT8148 was kindly provided by Dr. Nomura from the Department of Pediatric Dentistry of Osaka University Graduate School of Dentistry. Bacterial frozen glycerol stock was thawed and 100  $\mu$ L of suspension was cultured in 9.9 mL of Brain Heart Infusion Broth

(Becton, Dickinson and Company, Franklin Lakes, NJ, USA) with 1,500 µg/ml of streptomycin (Meiji Seika pharma Co., Ltd). After two passages, the bacteria were used for the infection. Briefly, the supernatant was discarded after the bacterial suspension was centrifugated at 3,000 rpm at 4°C for 10 min. Then, the bacterial pellet was washed with saline and centrifuged again. Finally, the bacterial pellets were resuspended in 10mL saline to obtain the final concentration of *S. mutans* suspension for inoculation.

### **c) Bacterial inoculation and cariogenic feeding**

The caries-induction timeline is shown in Fig. 1(a). At 18 days of age, the rats were infected with *S. mutans* by pipetting 200 µL of saline containing *S. mutans* suspension at approximately  $1 \times 10^8$  colony-forming units into the oral cavity. The infection procedure was performed for five consecutive days. After inoculation, the dental plaques were collected using sterilized cotton swabs and seeded in mitis salivarius-bacitracin (MSB) agar with the addition of 1,500 µg/ml streptomycin to confirm colony formation of *S. mutans*. The morphology of the colonies was confirmed by light microscopy (LED3000 NVI; Leika, Wetzlar, Germany). All animals were then fed with cariogenic “Diet 2000” powdered diet (sucrose 56%, wheat flour 7%) (CLEA Japan, Inc., Tokyo, Japan) *ad libitum* throughout the experimental period. In addition, the general hard feed crop was regularly fed to rats to make food easily impacted in the fissure of molars to accelerate caries induction.

### **2.1.2. Characterization of caries progression**

Caries progression was defined as shallow, moderate, and severe stages by evaluating the depth of the demineralized layer of dentin using micro-computed tomography (R-mCT2; Rigaku, Tokyo, Japan). The characterization of caries progression is shown in Fig. 1(b). Shallow caries was defined as a demineralized dentin layer less than outer 1/3 of the total thickness of dentin, moderate caries means radiolucency reaching between middle 1/3 of dentin and inner 1/3 of dentin, and severe stage means caries invasion to the inner 1/3 of dentin.

### **2.1.3. Histopathological evaluation**

#### **a) Tissue preparation**

Animals were euthanized once the caries lesion reached the prospective depth (e.g., shallow, moderate, or severe) through perfusion and fixation, as described previously [32, 33]. Briefly, the rats were intraperitoneally anesthetized and placed on an operating table. The thoracic cavity was opened to expose the heart and was held steady using forceps. The needle was directly inserted into the protrusion of the left ventricle to extend straight up about 5 mm and secured by a clamp near the entry. Next, the blood was removed using phosphate buffered saline (PBS) (Nacalai Tesque, Kyoto, Japan). Once all of the blood was cleared from the body, the solution was replaced with 4% paraformaldehyde phosphate buffer solution (Nacalai Tesque) for fixation. Perfusion was ceased once the jaw showed spontaneous minor movement and the color of the liver became lighter. The maxilla and mandible were collected

and fixed by immersion in the same fixative overnight at 4°C. Decalcification was performed by immersing the tissue in 0.1% ethylenediaminetetraacetic acid disodium salt and 4.3~5.3% hydrochloric acid (Karkitox, Fujifilm Wako Pure Chemical) for 3 days at 4°C. The teeth were dissected and embedded in paraffin using a paraffin embedding machine. Tissue blocks were trimmed into 5- $\mu$ m sections by microtome (RM 2155; Leica).

#### **b) H&E staining**

Hematoxylin and eosin (H&E) staining was performed to evaluate general inflammatory conditions under different caries progressions.

#### **c) Brown-Brenn staining**

To confirm whether bacteria invaded into the dentin and pulp, Brown-Brenn staining was performed as previously described [40]. Gram-positive bacteria can retain crystal violet staining (violet), while gram-negative bacteria take up the fuchsin stain and lose crystal violet stain as a result of the disruption of lipopolysaccharide during acetone rinse (pink).

#### **d) Immunohistochemical staining**

To determine whether pulpal inflammation was induced by caries, immunohistochemical staining was performed against Toll-like receptor 2, proliferating cell nuclear antigen, and double staining for CD68 and CD206. All sections were incubated in a DNA oven (MI-100; Kurabo, Osaka, Japan) at 56°C for



1 h before staining to prevent tissue detachment. After deparaffinization and rehydration, antigen retrieval was performed using citrate buffer (10 mM citric acid, pH 6.0) and incubated in the oven at 78°C for 20 min. The sections were washed with PBS after the buffer was returned to room temperature and incubated with 3% hydrogen peroxide (Kanto Chemical Co., Inc., Tokyo, Japan) diluted 10-fold with methanol (Kanto Chemical Co., Inc.) for endogenous peroxidase blocking. The ABC Kit (Vector Laboratories, Burlingame, CA, USA) was utilized for antigen detection according to the manufacturer's instructions. Rabbit anti-Toll-like receptor 2 polyclonal antibody (ab213676; Abcam, Cambridge, UK) at a dilution of 1:200 or rabbit anti-proliferating cell nuclear antigen polyclonal antibody (ab18197; Abcam) at a dilution of 1:1000 was used as the primary antibody. After biotinylated secondary antibody incubation, the tissue was further incubated with avidin conjugated with horseradish peroxidase (HRP). The HRP substrate was visualized by DAB staining kit (Vector laboratories) or ImmPACT NovaRed (Vector laboratories). The nuclei were counterstained with Mayer's Hematoxylin (Muto Pure Chemicals Co., Ltd, Tokyo, Japan).

For double immunofluorescence staining, the peroxidase blocking step was skipped. Unconjugated rabbit anti-mannose receptor CD206 polyclonal antibody (ab64693; Abcam) at a dilution of 1:500 was used as the primary antibody. After overnight incubation, the sections were probed with Alexa Fluor 488 conjugated goat anti-rabbit secondary antibody (ab150077; Abcam) at a dilution of 1:800 for 1 h. Alexa Fluor 594 conjugated rabbit anti-CD68 polyclonal antibody (bs-0649R-A594; Bioss, Woburn, MA, USA) at a dilution of 1:200 was used as the secondary primary antibody

after three washes with PBS. The sections were then mounted with Fluoroshield Mounting Medium with DAPI (Funakoshi Co., Ltd, Tokyo, Japan). All images were taken using an all-in-one fluorescence microscope (BZ-X800; Keyence Co., Osaka, Japan) and double positive signaling was assessed by BZ-X800 view analyzer software (Keyence).

## **2.2. Results**

### **2.2.1. Oral swab**

Bacterial colony formation was successfully observed on MSB agar (Fig. 2(a)). The colony morphology showed a rough granular surface that matched the profile of the *Streptococcus mutans* colony shape (Fig. 2(b)).

### **2.2.2. Micro-CT and hematoxylin and eosin staining**

The sagittal plane of micro-CT images of rat teeth under different carious progression is shown in Fig. 3(a), (e), and (i). The main focal area was determined in the demineralized layer near the mesial pulp horn to confirm caries progression according to the criteria described in Fig. 1(b). No radiolucent lesions were observed around the root apex in the shallow, moderate, and severe caries groups, which could indicate that the pulp tissue was not necrotic. To evaluate the holistic inflammatory status of the pulp at different stages of caries, the carious teeth were collected and stained with H&E. Representative images of H&E staining around the carious lesion are shown in

Fig. 3(b), (f), and (j). Abundant reactionary dentin was observed beneath the caries lesion in the moderate (Fig. 3(f)) and severe (Fig. 3(j)) caries groups. No significant reactionary dentin deposition was observed in the shallow caries group (Fig. 3(b)). In addition, significant cell infiltration was observed only in the severe caries group with the unarranged odontoblast layer (Fig. 3(j)).

### **2.2.3. Brown-Brenn staining**

Fig. 3(c), (g), and (k) show representative images of Brown-Brenn staining. No bacterial invasion was observed in any of the specimens of the dental pulp. Gram-positive bacteria were observed to invade the dentinal tubules in the moderate (Fig. 3(g)) and severe (Fig 3(k)) caries groups, while only the surface of the mesial fossa in the shallow caries group (Fig. 3(c)) showed negligible invasion by gram-positive bacteria.

### **2.2.4. Immunohistochemical staining**

To evaluate whether dental pulp was stimulated by caries progression, the distribution of Toll-like receptor 2 (TLR2) was investigated by immunohistochemical staining. The shallow caries group did not show a positive expression of TLR2 in dental pulp (Fig. 3(d)), which corresponds to the results of Brown-Brenn staining, as no bacteria were invading the dentinal tubules (Fig. 3(c)). The moderate caries group showed positive expression for TLR2 in the dental pulp, and some of the TLR2 positive cells were recruited close to the odontoblast layer beneath the caries lesion (Fig. 3(h)). In the severe caries group, the arrangement of odontoblasts was disrupted because of

persistent stimulation by caries, and abundant TLR2 positive cells were recruited beneath the carious lesion (Fig. 3(l)). Therefore, the pulpal inflammatory status in the moderate and severe caries groups was investigated in subsequent experiments.

The expression of proliferating cell nuclear antigen (PCNA) was investigated to evaluate the proliferative capacity of dental pulp cells under moderate and severe caries progression. Both groups showed PCNA-positive cells locally distributed in the dental pulp near the carious lesion (Fig. 4(a), (c)). Although the arrangement of the odontoblast layer remained intact, some PCNA-positive cells migrated to the odontoblast layer in the moderate caries group (Fig. 4(b)). In the severe group, the odontoblast layer was disrupted by caries progression, with abundant PCNA-positive cells recruited to the inflammatory site.

Furthermore, macrophage polarization in the inflamed dental pulp at different caries progression was also investigated (Fig. 5-7). CD68 (+) CD206 (-) cells are considered to be M1 macrophages, while CD68 (+) CD206 (+) cells are defined as M2 macrophages. In the moderate caries group, only a limited number of M1 macrophages were observed near the odontoblast layer, which was close to the carious lesion. In contrast, double-positive cells showed a relatively wider distribution compared to M1 macrophages in the pulp stimulated by the moderate carious lesion (Fig. 5(f)). In the severe caries group without pulp exposure, although the results showed there were some M2 macrophages distributed in the inflammation site, the main population of macrophage was M1 phenotype (Fig. 6(f)). In addition, to further differentiate the boundary between reversible and irreversible pulpitis, the macrophage population in the severe caries group with pulp exposure determined by

micro-CT was also investigated (Fig. 7). From immunofluorescence images, we found that abundant M1 macrophages accumulated just beneath the exposed site, yet no M2 macrophages were observed (white rectangle area of Fig. 7(f)). Some double-positive cells were observed only in the far region from the exposed site.

### **2.3. Discussion**

Innate immunity in the dentin-pulp complex is distinct from that in other tissues. It has a specific structure; the odontoblast layer, located in the outermost stratum of the dental pulp, not only has the capacity to secrete acquired dentin (reactionary dentin) to rescue the tooth from various external stimuli, but can also sense invading pathogens and elicit innate and/or adaptive immunity [41-44]. The occurrence of dental caries will precipitate the bacterial components invading through dentinal tubules and diffuse towards the peripheral pulp, causing the stimulation of odontoblasts to secrete cytokines and chemokines by activating their specific receptors, pathogen pattern recognition receptors (PRRs) [14,45]. Toll-like receptor 2 is a PRR that senses gram-positive bacterial components, such as lipoteichoic acid in odontoblasts [42, 45]. In this study, the inflammatory status of the pulp during caries progression was evaluated by immunohistochemical staining for TLR2, PCNA, and the observation of bacterial invasion in dentinal tubules by Brown-Brenn staining. The results of Brown-Brenn staining showed that gram-positive bacteria invaded the dentinal tubules only in the moderate and severe caries groups (Fig. 3(c, g, k)). The results of immunohistochemical staining also showed that TLR2 expression was

observed in the moderate and severe caries-stimulated pulp (Fig. (d, h, l)), suggesting that the immune response in dental pulp was successfully activated by moderate and severe carious invasion. Meanwhile, both moderate and severe caries groups showed PCNA-positive cell recruitment in the dental pulp beneath the carious lesion, but with different intensities (Fig. 4). PCNA is characterized as a DNA sliding clamp for replicative DNA polymerases and is an essential component of the eukaryotic chromosomal DNA replisome [46]. During the cell cycle, it has been reported that PCNA synthesis can be detected from the late G1 phase and reaches its maximum expression in the S phase [47]. We assume that such diversity in PCNA intensity is determined by proliferating cells with different cell cycle stages between moderate and severe caries. Besides that, it's been said the activation of TLR2 could be involved in NF- $\kappa$ B and MAPK signaling to regulate inflammation and repair processes [42, 48]. These results indicate that the positive expression of PCNA may be induced by the activation of TLR2 in the dental pulp for cell proliferation. We also observed that some PCNA-positive cells moved towards the odontoblast layer to replace the position of odontoblasts in the moderate caries group (Fig. 4(b)). Primary odontoblasts are terminally differentiated post-mitotic cells that are not replaced during the lifetime of the individuals [49], and many studies have illustrated that when odontoblasts encounter dentin irritation, they can activate apoptotic events [50, 51]. We assumed that the apoptosis of odontoblasts occurred under intensive carious stimuli and was replaced by newly differentiated odontoblast-like cells who expressed PCNA. These results suggest that the immune response of dental pulp was already activated by caries from the moderate stage, while it was not activated in the shallow carious stage.

As the phenotypic polarization of macrophages is mainly regulated by the surrounding microenvironment [52], we hypothesized that understanding the predominance of macrophage phenotype could help us to determine the inflammatory status of the pulp. The polarization of pro-inflammatory M1 macrophages is commonly induced by exposure to cytokines, such as interferon-gamma (IFN- $\gamma$ ), TNF- $\alpha$ , or bacterial cell components, lipoproteins, and TLR activators [21, 22, 53-55]. On the other hand, the polarization of anti-inflammatory M2 macrophages is produced by the interaction of cytokines, such as TGF- $\beta$ , IL-4, fungal/parasite complements, and apoptotic cells [21, 22, 53-55]. When investigating macrophage polarization in the inflamed pulp triggered by different progression of caries, the moderate caries group showed a dominant distribution of M2 macrophages (Fig. 5(f)), whereas the severe caries group showed M1 macrophage dominance (Fig. 6(f)). No M2 macrophages were observed beneath the exposure site in severe caries with pulp exposure (Fig. 7(f)). TGF- $\beta$ 2 has been shown to be present in mature dentin, which can be released from the dentin matrix and diffused to the pulp area when dental caries occurred [56, 57]. We propose that the release of TGF- $\beta$  from the dentin matrix may occur as a gradient, triggering the resident macrophages to polarize to the M2 phenotype in the early stage of dental caries. Meanwhile, when caries proceeded to the moderate stage, most of the odontoblasts maintained a densely packed structure, such that the bacterial product could be diffused to peripheral pulp tissue and mainly sensed by odontoblasts to regulate cytokine and chemokine secretion, which does not directly interact with immune cells such as macrophages [58]. We assumed the polarization of macrophages was mainly regulated by odontoblasts in the early pulpitis triggered by moderate caries when the odontoblast layer structure was not destroyed under carious stimuli.

An *in vitro* study by Farge *et al.* found that when odontoblasts were stimulated by gram-positive bacterial components, they would secrete less pro-inflammatory cytokines [59], which indicated that polarization to M1 macrophages may hardly be induced in the moderate caries group under gram-positive bacterial invasion. Furthermore, one clinical study investigated macrophage polarization in human carious teeth and reported M2 macrophage predominance in the caries stimulated pulp [60], which suggests that the inflammatory response in the rat caries model is comparable to that in human caries teeth. In addition, continued exposure to bacterial stimuli in severe carious teeth may lead to an alteration of the odontoblast layer [61], such that macrophages could directly interact with bacterial stimuli to induce phenotypic shift of M2 macrophages to M1 macrophages. The results of investigating macrophage polarization in the severe caries group could support this point of view (Fig. 6). Furthermore, monopolized M1 macrophages were observed in severe carious teeth with pulp exposure, while M2 macrophages, which play an anti-inflammatory role, were absent beneath the exposed site (Fig. 7(f)). Thus, we speculate that the predominance of M1 macrophages in the injured site may be the main cause of irreversible pulpitis.

In this chapter, our results showed that the immune response of dental pulp can be activated from the moderate stage of caries. This suggests that, to establish the caries induced pulpitis model, the carious lesion should be at least in the moderate carious stage of progression. Besides that, understanding the macrophage phenotype may help us to identify reversible (M2 dominant) and irreversible pulpitis (M1 dominant).



## **Chapter 3**

### **Tertiary dentin formation in caries-induced pulpitis model**

#### **3.1. Materials and Methods**

##### **3.1.1. Direct pulp capping procedure**

Direct pulp capping using ProRoot MTA (Dentsply-Sirona, York, PA, USA) was performed in moderate and severe carious teeth (n = 5) to evaluate tertiary dentin formation in the inflamed pulp. From the results of Chapter 2, moderate caries progression was considered reversible pulpitis, while the severe caries group indicated irreversible pulpitis. Non-infected sound teeth (n = 5) were used as control groups. The flow of the direct pulp-capping procedure is shown in Fig 1(c). Briefly, caries lesions were visualized by micro-CT before pulp capping, regardless of whether moderate or severe. During the procedure, infected dentin was examined using caries staining dye (Caries Detector, Kuraray Co, Osaka, Japan), and pulp exposure was intentionally occurred by a 0.5 mm round bur after complete caries removal in the moderate caries group. In the severe group, the pulp was unintentionally exposed during caries removal. The exposed pulp was irrigated with saline for 15 s, dried, capped with ProRoot MTA, and sealed with glass ionomer cement (Fuji IX, GC Corp, Tokyo, Japan) after confirmation of hemostasis.

### **3.1.2. Micro-CT analysis and histological analysis**

To determine whether an inflammatory reaction could affect the wound healing process, the volume of newly formed tertiary dentin 28 days after capping ( $n = 5$ ) was assessed by micro-CT, as previously described [62]. The data were reconstructed and quantitatively analyzed using three-dimensional reconstruction imaging software (TRI/3D-BON; Ratoc System Engineering, Japan) in moderate and sound groups. H&E staining was performed to evaluate the histological status of the tertiary dentin. The outcome of the wound healing process was determined by observing the structure of newly formed tertiary dentin, histological observation of the odontoblast-like layer, and presence of inflammatory cell infiltration.

## **3.2. Results**

### **3.2.1. Micro-CT analysis**

Micro-CT images revealed that complete tertiary dentin was formed in the sound and moderate caries groups 28 days after capping (Fig. 8(a), (d)). Incomplete hard tissue with defects was observed in the inferior area of the pulp chamber, away from the capping site in the severe caries group (Fig. 8(g)). We further investigated the volume of newly formed tertiary dentin beneath the capping site in the moderate and sound groups. Newly formed tertiary dentin exhibited less volume in the moderate caries group than in the sound group (Fig. 9(b),  $P < 0.05$ , Student's *t*-test,  $n = 5$ ), which indicates that the initial inflammation stimulated by caries may affect hard tissue

formation.

### **3.2.2. Hematoxylin and eosin staining**

Histological analysis by H&E staining also revealed that a complete tertiary dentin bridge was formed in the sound (Fig. 8(b)) and moderate caries (Fig. 8(e)) groups 28 days after pulp capping. Higher magnification of H&E images in the sound group showed arranged odontoblast-like layer beneath the newly formed dentin bridge with a clear similar direction to the dentinal tubular structure (Fig. 8(c)), whereas the moderate group showed an irregular direction of dentinal tubules with a lower arranged odontoblast-like layer (Fig. 8(f)). Meanwhile, the cell density showed differences between the sound and moderate groups, indicating that the pulp in the caries group may still be in the healing process. Incomplete hard tissue was observed in the severe caries group detached from the capping site, with the structure of cell infiltration into the calcified tissue, and the cell density was extremely high with strong eosin staining, indicating inflammation was not relieved beneath the calcified tissue (Fig. 8(i)).

### **3.3. Discussion**

The consensus mechanism of wound healing in dental pulp is when the injury occurs, after which mesenchymal stem cells (MSCs) are activated and migrate to the injured site, proliferate, and differentiate into odontoblastic-like cells to produce reparative tertiary dentin [63, 64]. In this study, the wound healing process under different

inflammatory statuses of pulp-healthy, reversible pulpitis, and irreversible pulpitis using a rat sound/caries model was investigated. The results showed that direct pulp capping in the healthy pulp exhibited an arranged odontoblast-like cell layer with a clear similar direction of the dentinal tubular structure in tertiary dentin (Fig. 8(c)). Direct pulp capping in the reversible pulpitis in the moderate caries group also showed newly formed tertiary dentin with an irregular non-continuous structure of dentinal tubules (Fig. (8f)), which correlates well with the clinical study of tertiary dentin formation in human carious teeth [65, 66]. This result further supported that moderate caries-induced inflammation of the pulp indicates reversible pulpitis. Many clinical studies have illustrated that the poorest quality of reparative dentin is usually associated with pulpal inflammation [61, 66]. Such tertiary dentin with irregular structure may be affected by the surrounding microenvironment of the injured site: pro-inflammatory cytokines released by immune cells, growth factors, the extent of cellular injury caused by hypoxia, and the state of differentiation of the replaced odontoblast-like cells, leading to adverse manifestations of mesenchymal stem cell function [15]. In contrast, incomplete hard tissue was observed in the severe caries group away from the capping site (Fig. 8(i)). The inflammation was not relieved beneath the calcified tissue, which indicated that the pulp status before treatment was irreversible. One study reported that the presence of M1 macrophages in the injured site leads to impaired healing and fibrosis [18]. Herein, the results obtained from the study of severe caries-induced pulpitis showed that M1 macrophages were predominant in the pulp tissue beneath the caries lesion (Fig. (6f)). We assume that when M1 macrophages become dominant in the dental pulp, although there may still be a chance to move to healing direction after pulp capping, the remaining M1

macrophages may induce MSC dysfunction, resulting in impaired wound healing. In addition, intensively eosin-stained pulp tissue indicated collagen deposition in the severe caries group, which may further cause pulp calcification (Fig. 8(i)). Considering the morphological specific structure and the formed region of calcified tissue found away from the capping area, we assumed that this hard tissue was not formed as a result of the healing process, but was rather caused by persistent inflammation in the severe group. These results indicate that the pulpal immune reaction could affect the structure of newly formed tertiary dentin, and severe inflammation could not be rescued by pulp capping using ProRootMTA.

We also investigated the volume of reparative tertiary dentin 28 days after pulp capping in teeth with caries-induced reversible pulpitis (moderate caries group) and healthy pulp using ProRoot MTA. A significantly higher volume of tertiary dentin was observed in the sound group than in the moderate caries group (Fig. 9B). The correlation between inflammatory conditions and activity of MSCs has been the subject of controversy in previous reports. Several studies found that under inflammatory and hypoxic conditions, the osteo/odontogenic differentiation ability of MSCs could be enhanced *in vitro* [67,68]. However, other studies reported that odontogenic differentiation of MSCs can be restricted under inflammatory conditions [69, 70]. MSCs derived from dental pulp possess similar multipotent potential as bone marrow-derived MSCs, including differentiation into odontoblast-like cells, cementoblasts, osteoblasts, chondrocytes, myocytes, epithelial cells, neural cells, hepatocytes, and adipocytes [70]. Therefore, the surrounding microenvironment in the injured site may play a vital role in determining the direction of MSCs differentiation.

In a clinical context, multiple factors can affect the precedence of MSC differentiation, as was mentioned in the previous sentence. The results showed that reparative tertiary dentin formation was downregulated even in reversible pulpitis treated with direct pulp capping compared with healthy pulp treated with direct pulp capping. We assume that the downregulation of tertiary dentin formation is caused by inflammation that affects the function of MSCs. However, more studies are needed to investigate the correlation between MSC behavior and inflammatory status. In addition, the tubular structure of the tertiary dentin may be another factor affecting hard tissue deposition by odontoblastic-like cells. In the absence of regular tubular structure, newly differentiated cells have difficulty receiving signals from stimuli, which may decrease hard tissue formation in the carious tooth.

These results suggest that the deposition of hard tissue formation should not be the only evaluation standard in the wound healing process of dental pulp, as immune reactions may affect the structure of newly formed tertiary dentin. Meanwhile, together with the results presented in Chapter 2, we suggest using moderate caries progression, characterized by a predominance of M2 macrophages in inflamed pulp, as a reversible pulpitis model for direct pulp capping. Moreover, controlling macrophage polarization may provide new clinical therapeutic strategies for irreversible pulpitis. Further studies will be needed to precisely determine the correlation between macrophage and mesenchymal activity under various inflammatory conditions.

## **Chapter 4**

# **Assessment of inflammatory changes during wound healing process in reversible pulpitis after pulp capping with ProRoot MTA**

### **4.1. Materials and Methods**

#### **4.1.1. Animal experiments and histological analysis**

To investigate the inflammatory changes during the wound healing process in moderate carious-stimulated dental pulp, which is considered to be reversible pulpitis, double immunofluorescent staining of CD68 and CD206 was performed to monitor the spatiotemporal localization of macrophages on days 1, 3, 7, and 14 post-capping, with the previously described methods in Chapter 2 and 3. The cell proliferative capacity was also investigated by immunohistochemical staining for PCNA at the same point in time. H&E staining was performed to evaluate the histological changes during wound healing. Sound teeth were used as controls.

#### **4.1.2. Quantification of relative numbers of positive cells**

The double-positive cells for CD68 and CD206 (n = 5) and PCNA-positive cells (n = 3) at each time point were quantified using ImageJ Fiji (NIH, <https://imagej.net/software/fiji/>).

### **4.1.3. Statistical analysis**

The statistical significance of double positive cells ( $n = 5$ ) and PCNA expression ( $n = 3$ ) at different time points in the moderate caries and sound groups were measured using one-way ANOVA and Tukey's HSD test. The positive cell numbers of M2 macrophages and PCNA at the same time points between the caries and sound groups was further measured by Student's *t*-test. All tests were performed using IBM SPSS Statistics 22 (International Business Machines Corp., Armonk, NY, USA). Statistical significance was set at  $P < 0.05$ .

## **4.2. Results**

### **4.2.1. H&E staining**

H&E staining was performed at 1, 3, 7, and 14 days post-capping to evaluate the histological changes during the wound healing process. In the sound group, inflammatory cell infiltration was limited beneath the cavity on days 1 and 3, and the residual pulp tissue away from the exposure remained under normal conditions with no significant cell infiltration (Fig. 10(e), (f)). On the contrary, cell density was high in the entire pulp area on days 1 and 3 in the moderate caries group (Fig. 10(a), (b)). However, both groups showed a similar tendency of tertiary dentin formation; the connective tissue started to form on day 3, while partial tertiary dentin was formed on day 7, and dentin formation complete on day 14.



#### 4.2.2. Double immunofluorescence staining

To further investigate the inflammatory changes during the wound healing process of reversible pulpitis, the spatiotemporal polarization of macrophages was investigated in the moderate caries group after pulp capping. Direct pulp capping in the sound tooth was used as the control group. In the moderate caries group, only limited M1 macrophages were observed beneath the capping site on day 1 (Fig. 11A(a)), whereas M2 macrophages were predominant at each time point after capping (Fig. 11A(a-d)). In addition, M2 macrophages exhibited a distinct shift in cell numbers during the wound healing process in the moderate caries-stimulated pulp. The maximum population of M2 macrophages was observed on day 3 and started to decrease after day 7 in the moderate caries group ( $P < 0.05$ ) (Fig. 11B). In the sound group, the population of M2 macrophages was relatively low compared with the caries group at each time point (Fig. 12A(a-d)). No significant changes in the M2 macrophage population were observed in the sound group throughout the experimental period ( $P > 0.05$ ) (Fig. 12B).

We also compared the number of double-positive M2 macrophages between the moderate caries and sound groups at each time point to determine whether the initial pulpal inflammation caused by caries could affect the macrophage population during the wound healing process. The results showed that the population of M2 macrophages was significantly higher on days 1 and 3 in the caries group ( $P < 0.05$ ) (Fig. 13(a), (b)).

### **4.2.3. Immunohistochemical staining of PCNA**

We investigated the transition of the proliferative capacity of dental pulp during the wound healing process via the immunohistochemical staining of proliferating cell nuclear antigen on days 1, 3, 7, and 14 post-capping. Representative images showed that a wide distribution of PCNA-positive cells was found in the moderate caries group on days 1, 3, and 7 (Fig. 14(a-c)), whereas PCNA-positive cells were distributed in a limited area close to the capping site in the sound group (Fig. 14(e-h)). Next, we performed an image quantitative analysis to evaluate PCNA expression in these two groups ( $n = 3$ ). PCNA expression in the moderate caries group showed abundant expression on day 3 ( $P < 0.05$ ), decreased from day 7 (Fig. 15A), while no significant differences were found throughout the time points in the sound group ( $P > 0.05$ ) (Fig. 15B). To investigate whether the proliferation capacity was affected by inflammation, we further compared PCNA expression between the sound and caries groups. The caries group showed significantly higher expression on day 3 compared to the sound group ( $P < 0.05$ ) (Fig. 16).

### **4.3. Discussion**

To investigate the transition of inflammatory conditions during the wound healing process, the spatial temporal localization of macrophages was investigated. Macrophages play an essential role in the healing of numerous tissues [18, 19, 21, 22], promoting the debridement of injured tissue, cell proliferation, angiogenesis, collagen

deposition, and matrix remodeling by controlling the polarization of multifunctional phenotypes of macrophages [71]. M1 phenotype is predominant in the inflammatory phase and plays a scavenger function, while M2 phenotype is predominant during the proliferative and remodeling phases [18]. In this study, M2 macrophages were predominant at all time points after pulp capping (Fig. 11A), which did not match the general phenotypic transition of macrophages during the wound healing process. Since dental pulp can sense bacterial invasion before it reaches the pulp area [41-43], defending action has already started. Thus, the results of histological evaluation in caries model showed that the reversible pulpitis triggered by moderate caries was already filled with M2 macrophages before treatment (Fig. 5(f)). Furthermore, proliferating cells were also observed under moderate caries progression (Fig. 4). Therefore, the process of inflammation and proliferative phases was highly overlapped and took place before we performed direct pulp capping in the inflamed pulp. When direct pulp capping was performed in moderate caries-induced reversible pulpitis, the main population of macrophages in the injury site still became those of the M2 phenotype. The phenotypic shift of M2 to M1 macrophages was considered to occur in response to microenvironmental cues, such as LPS, TNF- $\alpha$  [72]. We assumed that if infection was thoroughly controlled at the exposure site, the phenotypic transition would be negligibly induced upon pulp capping in reversible pulpitis. However, if not, the remaining carious stimuli in exposure could also induce the pulp to become irreversible by phenotypic transition from M2 to M1 macrophages.

Although we did not observe the phenotypic transition of macrophages, the quantitative investigation of the M2 macrophage population showed that there was a

significant shift in the M2 macrophage population during the wound healing process (Fig. 11B), while no such changes were observed after pulp capping in the sound group (Fig. 12B). These results suggest that the healing process in caries-induced reversible pulpitis may vary from that of healthy pulp with mechanical exposure, which is likely to be mainly regulated by M2 macrophages. By observing the number of M2 macrophages between the moderate caries group and the sound group at different time points, we found that only day 1 and day 3 were significantly different ( $P < 0.05$ ) (Fig. 13). This indicates that the inflammatory response stimulated by caries could affect the early stage of wound healing by regulating the M2 macrophage population. However, more studies are needed to fully elucidate the role of M2 macrophages during wound healing.

The transition of proliferative capacity in moderate carious-induced reversible pulpitis treated with direct pulp capping was investigated. PCNA-positive cells showed a peak population on day 3 ( $P < 0.05$ ) and started to decrease after day 7 in the moderate caries group (Fig. 15A). In contrast, no significant differences were observed in the sound group among the experimental time points ( $P > 0.05$ ) (Fig. 15B). These results indicate that the pulp underwent a more complex inflammatory-healing process under inflammatory conditions stimulated by caries. M2 macrophages have been reported to upregulate MSC proliferation and migration at the site of wounds [73, 74]. Compared with the sound group, we observed that the inflamed pulp had a significantly higher population of M2 macrophages in the early stage of wound healing (Fig. 13), which may result in an upregulation of proliferative capacity in the pulp. In addition, the shift in the number of M2 macrophages was similar to that of

PCNA expression during the wound healing process in reversible pulpitis. It has been reported that macrophages are willing to proliferate locally rather than recruit monocytes to the injury site [75]. We assume that, apart from the upregulation of mesenchymal stem cell proliferation, macrophage self-proliferation also contributes to inflammation. Further studies will be needed to elucidate the specific regulation of M2 macrophages during the wound healing process under inflammatory conditions.

## **Chapter 5**

### **Conclusions**

In summary, we successfully established a caries-induced pulpitis model for direct pulp capping. M2 macrophages play an important role in the early stages of the wound healing process of reversible pulpitis.

1. TLR2 expression was observed in the moderate and severe caries groups, but not in the shallow caries groups. Both the moderate and severe caries groups showed positive PCNA expression beneath the caries lesion. The polarization of macrophage type was discriminated between the two groups. Moderate caries showed an M2-dominant distribution, whereas the severe caries group showed M1 dominance.
2. Pulp capping in moderate carious teeth is considered to be reversible pulpitis, showing complete tertiary dentin formation 28 days post-treatment. Impaired wound healing was observed in the severe caries group, which was considered to be irreversible pulpitis.
3. M2 macrophages were predominant throughout the whole period of wound healing process in reversible pulpitis, and the proliferative capacity was upregulated in the early stage of wound healing compared to healthy pulp.

## Chapter 6

### References

1. C Yu, P V Abbott. 2007. An overview of the dental pulp: its functions and responses to injury. *Aust Dent J.* 52(1 Suppl): S4-16.
2. TJ Hilton. 2009. Keys to clinical success with pulp capping: a review of the literature. *Oper Dent.* 34(5): 615–625.
3. Ghoddusi J, Forghani M, Parisay I. 2014. New approaches in vital pulp therapy in permanent teeth. *Iran Endod J.* 9(1): 15–22.
4. Song M, Yu B, Kim S, Hayashi M, Smith C, Sohn S, Kim E, Lim J, Stevenson RG, Kim RH. 2017. Clinical and molecular perspectives of reparative dentin formation: lessons learned from pulp-capping materials and the emerging roles of calcium. *Dent Clin North Am.* 61(1): 93–110.
5. Baume L, Holz J. 1981. Long-term clinical assessment of direct pulp capping. *Int Dent J.* 31(4): 251–260.
6. Al-Hiyasat A.S, Barrieshi-Nusair K.M, Al-Omari M. 2006. The radiographic outcomes of direct pulp-capping procedures performed by dental students: a retrospective study. *J Am Dent Assoc.* 137(12): 1699–1705.
7. PV Abbott, C Yu. 2007. A clinical classification of the status of the pulp and the root canal system. *Aust Dent J.* 52:(1 Suppl): S17-S31.

8. Ricucci D, Loghin S, Siqueira JF Jr. 2014. Correlation between clinical and histologic pulp diagnoses. *J Endod.* 40(12): 1932-9.
9. Mejàre IA, Axelsson S, Davidson T, Frisk F, Hakeberg M, Kvist T, Norlund A, Petersson A, Portenier I, Sandberg H, Tranaeus S, Bergenholtz G. 2012. Diagnosis of the condition of the dental pulp: a systematic review. *Int Endod J.* 45(7): 597-613.
10. Rechenberg DK, Galicia JC, Peters OA. 2016. Biological markers for pulpal inflammation: a systematic review. *PLoS One.* 11(11): e0167289.
11. Michaelson P, Holland G. 2002. Is pulpitis painful. *Int Endod J.* 35: 829–832.
12. Dummer PM, Hicks R, Huws D. 1980. Clinical signs and symptoms in pulp disease. *Int Endod J.* 13: 27–35.
13. Zanini M, Meyer E, Simon S. 2017. Pulp inflammation diagnosis from clinical to inflammatory mediators: a systematic review. *J Endod.* 43(7): 1033-1051.
14. Hahn CL, Liewehr FR. 2007. Innate immune responses of the dental pulp to caries. *J Endod.* 33(6): 643-651.
15. Guo S, Dipietro LA. 2010. Factors affecting wound healing. *J Dent Res.* 89(3): 219–229.
16. Landén NX, Li D, Stähle M. 2016. Transition from inflammation to proliferation: a critical step during wound healing. *Cell Mol Life Sci.* 73(20): 3861–3885.
17. Ploeger DT, Hosper NA, Schipper M, Koerts JA, de Rond S, Bank RA. 2013. Cell plasticity in wound healing: paracrine factors of M1/ M2 polarized macrophages



- influence the phenotypical state of dermal fibroblasts. *Cell Commun Signal.* 11(1): 29.
18. Paulina K, Rene Ss, Andre P, François B. 2018. The role of macrophages in acute and chronic wound healing and interventions to promote pro-wound healing phenotypes. *Front Physiol.* 9: 419.
19. Rószter T. 2015. Understanding the mysterious M2 macrophage through activation markers and effector mechanisms. *Mediators Inflamm.* 2015:816460.
20. Neves VCM, Yianni V, Sharpe PT. 2020. Macrophage modulation of dental pulp stem cell activity during tertiary dentinogenesis. *Sci Rep.* 10(1): 20216.
21. Mosser DM, Hamidzadeh K, Goncalves R. 2021. Macrophages and the maintenance of homeostasis. *Cell Mol Immunol.* 18(3): 579-587.
22. Krzyszczyk P, Schloss R, Palmer A, Berthiaume F. 2018. The role of macrophages in acute and chronic wound healing and interventions to promote pro-wound healing phenotypes. *Front Physiol.* 9:419.
23. Bruno KF, Silva JA, Silva TA, Batista AC, Alencar AH, Estrela C. 2010. Characterization of inflammatory cell infiltrate in human dental pulpitis. *Int Endod J.* 43(11): 1013-21.
24. Lee S, Zhang QZ, Karabucak B, Le AD. 2016. DPSCs from inflamed pulp modulate macrophage function via the TNF- $\alpha$ /IDO axis. *J Dent Res.* 95(11): 1274–1281.

25. Caviedes-Bucheli J, Moreno GC, López MP, Bermeo-Noguera AM, Pacheco-Rodríguez G, Cuellar A, Muñoz HR. 2008. Calcitonin gene-related peptide receptor expression in alternatively activated monocytes/macrophages during irreversible pulpitis. *J Endod.* 34(8): 945-949.
26. Dammaschke T. 2010. Rat molar teeth as a study model for direct pulp capping research in dentistry. *Lab. Anim.* 44: 1-6.
27. He Y, Gan Y, Lu J, Feng Q, Guan H, Jiang Q. 2017. Pulpal tissue inflammatory reactions after experimental pulp exposure in mice. *J Endod.* 43(1): 90-95.
28. Aubeux D, Renard E, Pérez F, Tessier S, Geoffroy V, Gaudin A. 2021. Review of animal models to study pulp inflammation. *Front. Dent. Med.* 2021: 673552
29. Shi X, Li Z, He Y, Jiang Q, and Yang X. 2017. Effect of different dental burs for experimental induction of pulpitis in mice. *Arch Oral Biol.* 83: 252–7.
30. Chung MK, Lee J, Duraes G, and Ro JY. 2011. Lipopolysaccharide-induced pulpitis up-regulates TRPV1 in trigeminal ganglia. *J Dent Res.* 90: 1103–7.
31. Hall BE, Zhang L, Sun ZJ, Utreras E, Prochazkova M, Cho A, et al. 2016. Conditional TNF- $\alpha$  overexpression in the tooth and alveolar bone results in painful pulpitis and osteitis. *J Dent Res.* 95:188–195.
32. Okamoto M, Takahashi Y, Komichi S, Cooper PR, Hayashi M. 2018. Dentinogenic effects of extracted dentin matrix components digested with matrix metalloproteinases. *Sci Rep.* 8: 0690.
33. Komichi S, Takahashi Y, Okamoto M, Ali M, Watanabe M, Huang H, Nakai T,

- Cooper P, Hayashi M. 2019. Protein S100-A7 derived from digested dentin is a critical molecule for dentin pulp regeneration. *Cells*. 8(9): 1002.
34. Loesche WJ. 1986. Role of *Streptococcus mutans* in human dental decay. *Microbiol Rev*. 50(4): 353-380.
35. Cheyne VD. 1940. Inhibition of experimental dental caries by fluorine in the absence of saliva. *Proc Soc Exp Biol Med*. 43: 58–61.
36. Bowen WH. 2013. Rodent model in caries research. *Odontology*. 101(1): 9-14.
37. Neves Ade A, Coutinho E, Vivan Cardoso M, Jaecques SV, Van Meerbeek B. 2010. Micro-CT based quantitative evaluation of caries excavation. *Dent Mater*. 26(6): 579-588.
38. Yucesoy DT, Fong H, Gresswell C, Saadat S, Chung WO, Dogan S, Sarikaya M. 2018. Early caries in an in vivo model: structural and nanomechanical characterization. *J Dent Res*. 97(13): 1452-1459.
39. Ooshima T, Minami T, Matsumoto M, Fujiwara T, Sobue S, Hamada S. 1998. Comparison of the cariostatic effects between regimens to administer oolong tea polyphenols in SPF rats. *Caries Res* 32: 75–80.
40. Hirose N, Kitagawa R, Kitagawa H, Maezono H, Mine A, Hayashi M, Haapasalo M, Imazato S. 2016. Development of a cavity disinfectant containing antibacterial monomer MDPB. *J Dent Res*. 95(13): 1487-1493.
41. Farges JC, Alliot-Licht B, Renard E, Ducret M, Gaudin A, Smith AJ, Cooper PR. 2015. Dental pulp defence and repair mechanisms in dental caries. *Mediators*

- Inflamm. 2015: 230251.
42. Farges JC, Keller JF, Carrouel F, Durand SH, Romeas A, Bleicher F, Lebecque S, Staquet MJ. 2009. Odontoblasts in the dental pulp immune response. *J Exp Zool B Mol Dev Evol.* 312(5): 425–436.
  43. Hahn CL, Liewehr FR. 2007. Innate immune responses of the dental pulp to caries. *J Endod.* 33(6): 643–651.
  44. Veerayutthwilai O, Byers MR, Pham TT, Darveau RP, Dale BA. 2007. Differential regulation of immune responses by odontoblasts. *Oral microbiol. immunol.* 22(1): 5–13.
  45. Yumoto H, Hirao K, Hosokawa Y, Kuramoto H, Takegawa D, Nakanishi T, Matsuo T. 2018. The roles of odontoblasts in dental pulp innate immunity. *Jpn Dent Sci Rev.* 54(3): 105-117.
  46. Maga G, Hubscher U. 2003. Proliferating cell nuclear antigen (PCNA): a dancer with many partners. *J Cell Sci.* 116(Pt 15): 3051-3160.
  47. Suzuki K, Hemmi A, Katoh R, Kawaoi A. 1996. Differential image analysis of proliferating cell nuclear antigen (PCNA) expression level during experimental thyroid carcinogenesis. *Acta Histochem. Cytochem.* 29(2): 99-105.
  48. Li X, Jiang S, Tapping RI. 2010. Toll-like receptor signaling in cell proliferation and survival. *Cytokine.* 49(1): 1–9.
  49. Ruch JV, Lesot H, Bègue-Kirn C. 1995. Odontoblast differentiation. *Int J Dev Biol.* 39(1): 51-68.

50. Mitsiadis TA, De Bari C, About I. 2008. Apoptosis in developmental and repair-related human tooth remodeling: a view from the inside. *Exp Cell Res.* 314(4): 869-877.
51. Wang HS, Pei F, Chen Z, Zhang L. 2016. Increased apoptosis of inflamed odontoblasts is associated with CD47 loss. *J Dent Res.* 95(6): 697-703.
52. Atri C, Guerfali FZ, Laouini D. 2018. Role of human macrophage polarization in inflammation during infectious diseases. *Int J Mol Sci.* 19(6): 1801.
53. Wang N, Liang H, Zen K. 2014. Molecular mechanisms that influence the macrophage M1–M2 polarization balance. *Front Immunol.* 5: 614.
54. Mosser DM, Edwards JP. 2008. Exploring the full spectrum of macrophage activation. *Nat Rev Immunol.* 8(12): 958–969.
55. Murray PJ, Wynn TA. 2011. Obstacles and opportunities for understanding macrophage polarization. *J Leukoc Biol.* 89(4): 557–563.
56. Finkelman RD, Mohan S, Jennings JC, Taylor AK, Jepsen S, Baylink D. 1990. Quantitation of growth factors IGF-1, SGF/IGF-11 and TGF- $\beta$  in human dentin. *J Bone Miner Res.* 5: 717–723.
57. Sloan AJ, Perry JB, Matthews JB, Smith AJ. 2000. Transforming growth factor-beta isoform expression in mature human healthy and carious molar teeth. *Histochem J.* 32: 247–252.
58. Galler KM, Weber M, Korkmaz Y, Widbiller M, Feuerer M. 2021. Inflammatory response mechanisms of the dentine–pulp complex and the periapical tissues. *Int*

J Mol Sci. 22(3): 1480.

59. Farges JC, Carrouel F, Keller JF, Baudouin C, Msika P, Bleicher F, Staquet MJ. 2011. Cytokine production by human odontoblast-like cells upon Toll-like receptor-2 engagement. *Immunobiology*. 216(4): 513-517.
60. Yoshiba N, Edanami N, Ohkura N, Maekawa T, Takahashi N, Tohma A, Izumi K, Maeda T, Hosoya A, Nakamura H, Tabeta K, Noiri Y, Yoshiba K. 2020. M2 phenotype macrophages colocalize with schwann cells in human dental pulp. *J Dent Res*. 99(3): 329-338.
61. Ricucci D, Loghin S, Niu LN, Tay FR. 2018. Changes in the radicular pulp-dentine complex in healthy intact teeth and in response to deep caries or restorations: A histological and histobacteriological study. *J Dent*. 73: 76-90.
62. Okamoto M, Takahashi Y, Komichi S, Ali M, Yoneda N, Ishimoto T, Nakano T, Hayashi M. 2018. Novel evaluation method of dentin repair by direct pulp capping using high-resolution micro-computed tomography. *Clin Oral Investig*. 22(8): 2879-2887.
63. Nakashima M, Akamine A. 2005. The application of tissue engineering to regeneration of pulp and dentin in endodontics. *J Endod*. 31: 711–718.
64. Shah D, Lynd T, Ho D, Chen J, Vines J, Jung HD, Kim JH, Zhang P, Wu H, Jun HW, Cheon K. 2020. Pulp–dentin tissue healing response: a discussion of current biomedical approaches. *J Clin Med*. 9(2): 434.
65. Ricucci D, Loghin S, Lin LM, Spångberg LS, Tay FR. 2014. Is hard tissue formation in the dental pulp after the death of the primary odontoblasts a

- regenerative or a reparative process? *J Dent.* 42(9): 1156-1170.
66. Trowbridge HO. 1981. Pathogenesis of pulpitis resulting from dental caries. *J Endod.* 7(2): 52-60.
67. Croes M, Oner FC, Kruyt MC, Blokhuis TJ, Bastian O, Dhert WJ, Alblas J. 2015. Proinflammatory mediators enhance the osteogenesis of human mesenchymal stem cells after lineage commitment. *PLoS One.* 10(7): e0132781.
68. Croes M, Kruyt MC, Loozen L, Kragten AH, Yuan H, Dhert WJ, Öner FC, Alblas J. 2017. Local induction of inflammation affects bone formation. *Eur Cell Mater.* 33: 211-226.
69. Wang F, Jiang Y, Huang X, Liu Q, Zhang Y, Luo W, Zhang F, Zhou P, Lin J, Zhang H. 2017. Pro-inflammatory cytokine TNF- $\alpha$  attenuates BMP9-induced osteo/ odontoblastic differentiation of the stem cells of dental apical papilla (SCAPs). *Cell Physiol Biochem.* 41(5): 1725-1735.
70. Li B, Ouchi T, Cao Y, Zhao Z, Men Y. 2021. Dental-derived mesenchymal stem cells: state of the art. *Front. Cell Dev. Biol.* 9: 654559.
71. Novak ML, Koh TJ. 2013. Phenotypic transitions of macrophages orchestrate tissue repair. *Am J Pathol.* 183(5): 1352-1363.
72. Shapouri-Moghaddam A, Mohammadian S, Vazini H, Taghadosi M, Esmaeili SA, Mardani F, Seifi B, Mohammadi A, Afshari JT, Sahebkar A. 2018. Macrophage plasticity, polarization, and function in health and disease. *J Cell Physiol.* 233(9): 6425-6440.

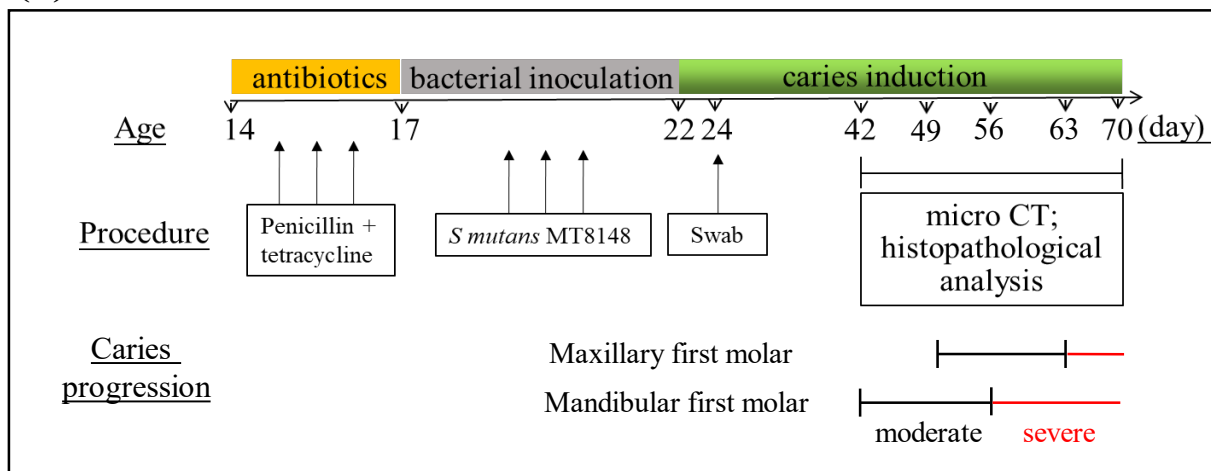
73. Yu, B., Sondag, G. R., Malcuit, C., Kim, M. H., and Safadi, F. F. 2016. Macrophage-associated osteoactivin/GPNMB mediates mesenchymal stem cell survival, proliferation, and migration via a CD44-dependent mechanism. *J. Cell Biochem.* 117(7): 1511-1521.
74. Xia, Y., He, X. T., Xu, X. Y., Tian, B. M., An, Y., and Chen, F. M. 2020. Exosomes derived from M0, M1 and M2 macrophages exert distinct influences on the proliferation and differentiation of mesenchymal stem cells. *PeerJ.* 8: e8970.
75. Jenkins SJ, Ruckerl D, Cook PC, Jones LH, Finkelman FD, van Rooijen N, MacDonald AS, Allen JE. 2011. Local macrophage proliferation, rather than recruitment from the blood, is a signature of Th2 inflammation. *Science.* 332(6035): 1284–1288.



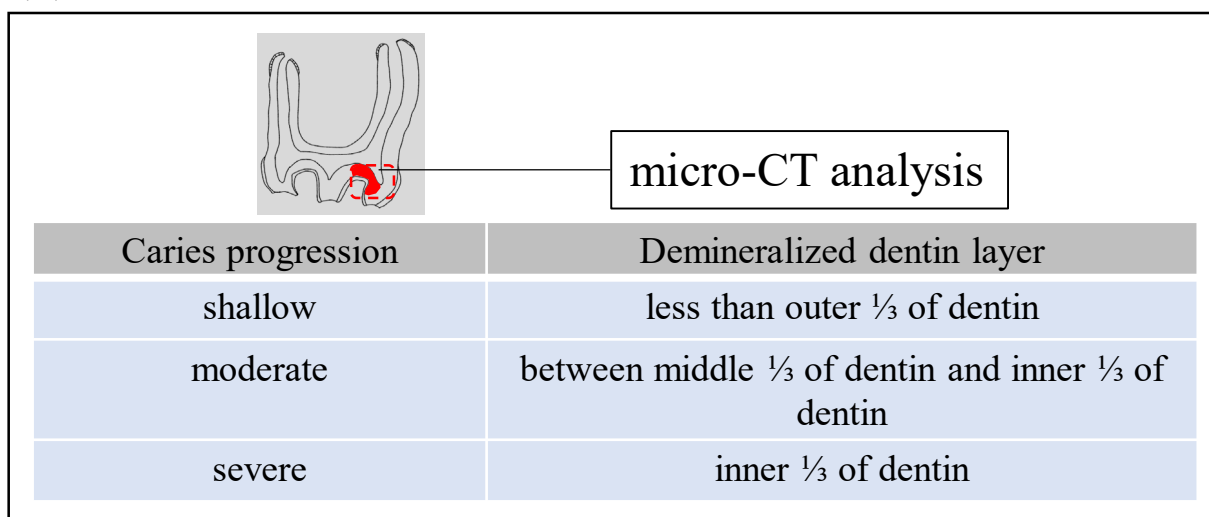
## **Chapter 7**

### **Figures and Tables**

(a)



(b)



(c)

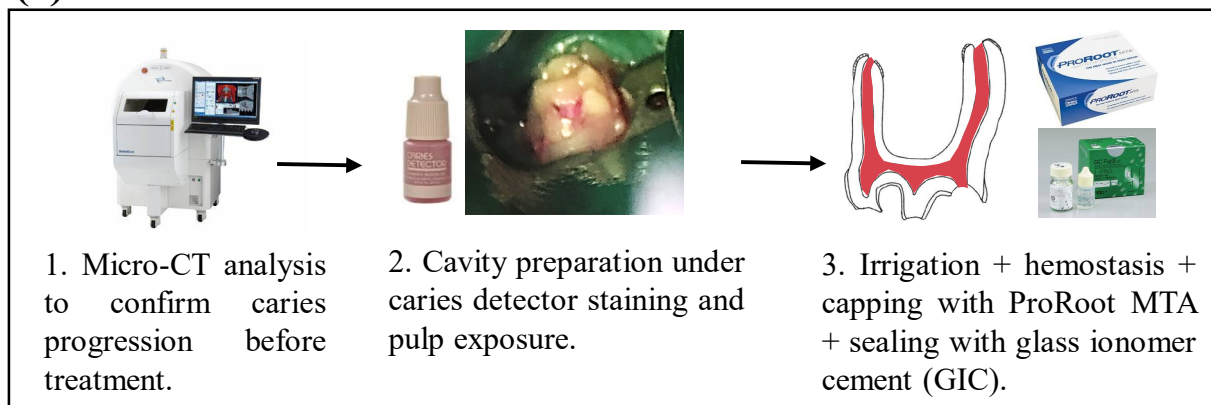


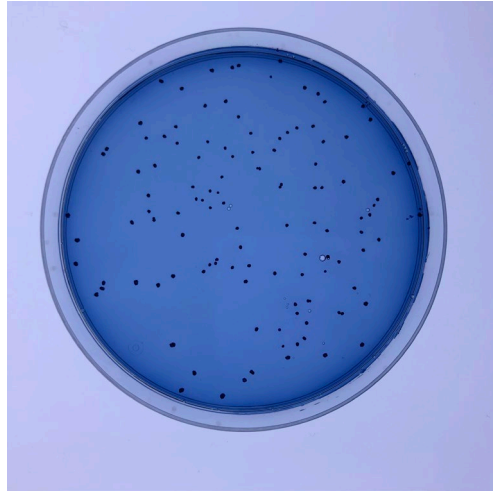
**Figure 1. Schematic diagram of experimental protocol.**

(a): Caries induction timeline.

(b): Classification of the caries progression by micro-CT.

(c): Direct pulp capping procedure.

**(a)**



**(b)**

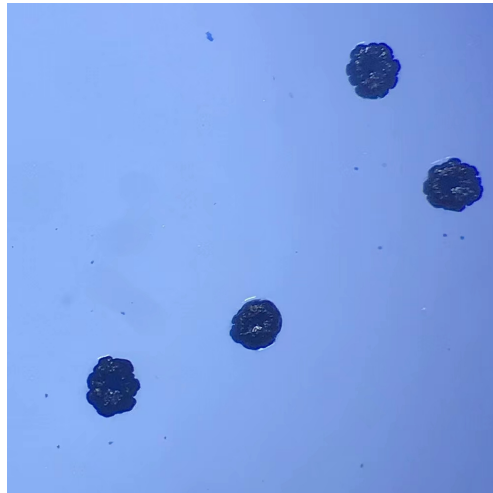


**Figure 2. Photo images of oral swab.**

(a): Representative image of bacterial colony formation on mitis salivarius bacitracin (MSB) agar plate.

(b): Microscopic observation of bacterial colony morphology. The colony morphology showed a rough granular surface that matched the profile of *Streptococcus mutans* colony.

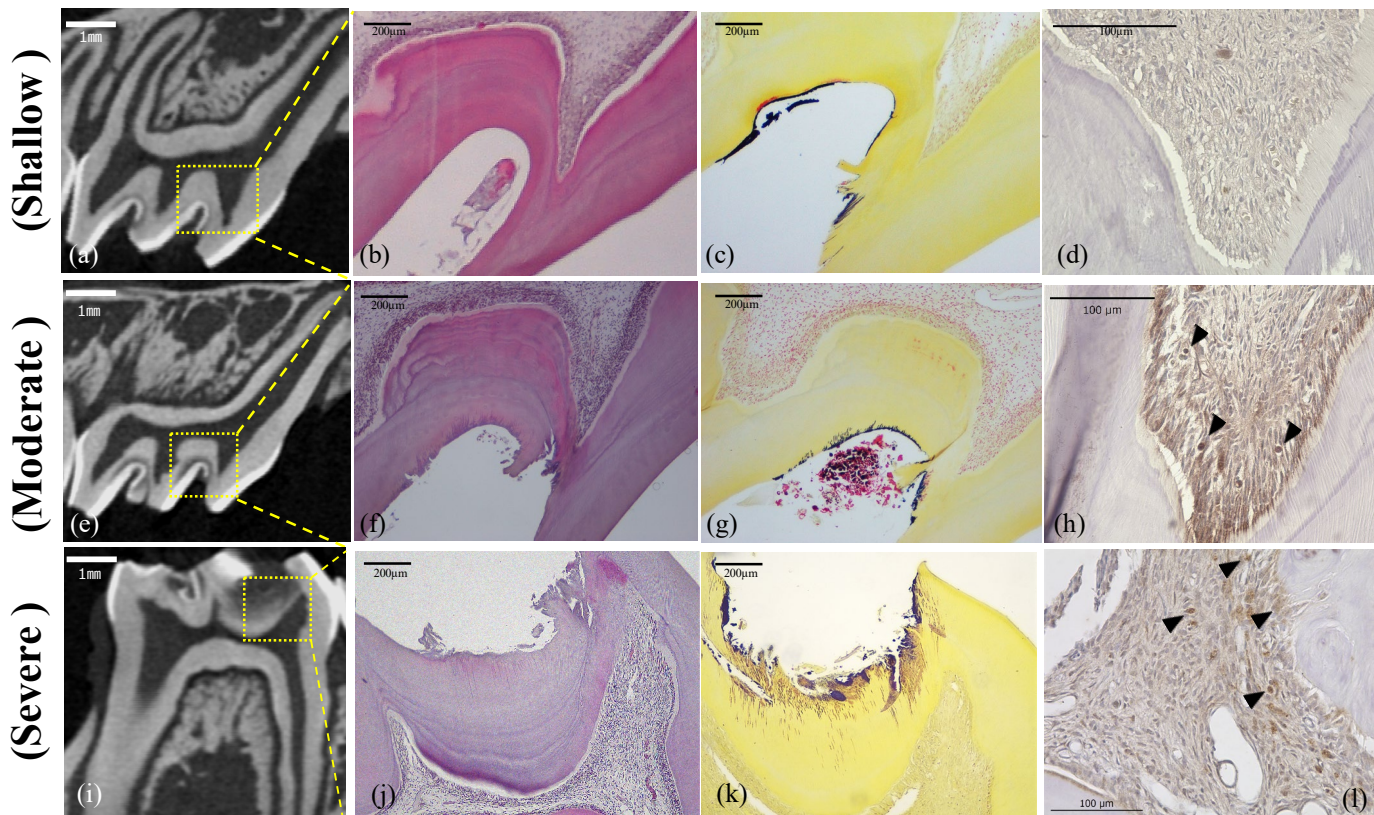


**Figure 3. Pulp status under different carious progression.**

Representative images of micro-CT in the sagittal plane under different carious progression (a, e, i). H&E staining images (b, f, j) show reactionary dentin formed beneath the caries lesion in the moderate (f) and severe (j) groups, but was not found in shallow group (b). Only the severe group showed severe inflammatory cell infiltration (j). Representative images of Brown-Brenn staining (c, g, k) show bacterial invasion through dentinal tubules in the moderate (g) and severe (k) groups. The immunohistochemical staining of toll-like receptor 2 (TLR2) (d, h, l) indicated that TLR2 was not expressed in the shallow caries group (d). Some of the TLR2 positive cells were recruited to the odontoblast layer near the caries lesion in the moderate group (h). Abundant TLR2 positive cells were recruited beneath the carious lesion in the severe group (l). The yellow rectangles in the micro-CT denote enlarged sites. Black arrowheads indicate TLR2 positive cells.

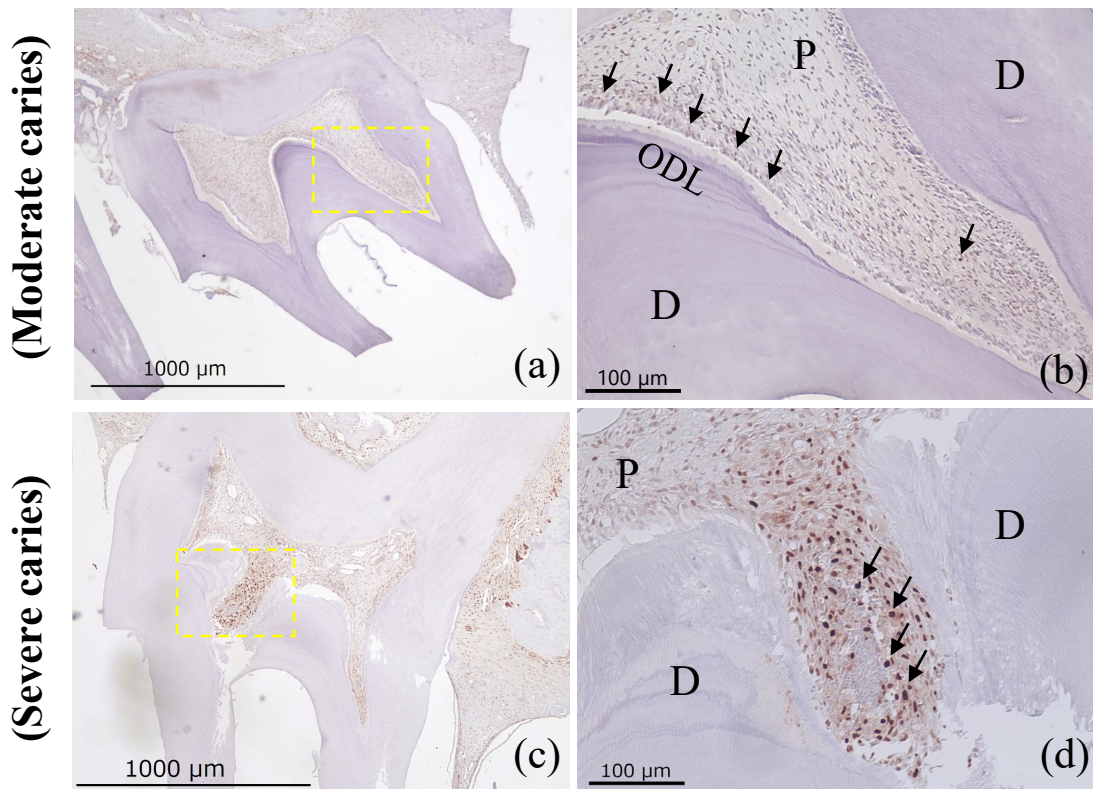


**Figure 4. Immunohistochemical staining for proliferating cell nuclear antigen (PCNA) under moderate and severe carious progression.**

Immunohistochemical staining of PCNA under low (a, c) and high (b, d) magnification of moderate (a, b) and severe caries (c, d). Both groups showed positive expression of PCNA in dental pulp (a, c). Higher magnification shows that some PCNA (+) cells were recruited to the odontoblastic layer beneath the caries lesion in moderate caries (b). Intensive positive expression of PCNA was observed beneath the caries lesion in severe caries (d). D: dentin; P: pulp; ODL: odontoblastic layer; Arrow: PCNA (+) cells; The yellow rectangle shows an enlarged site.

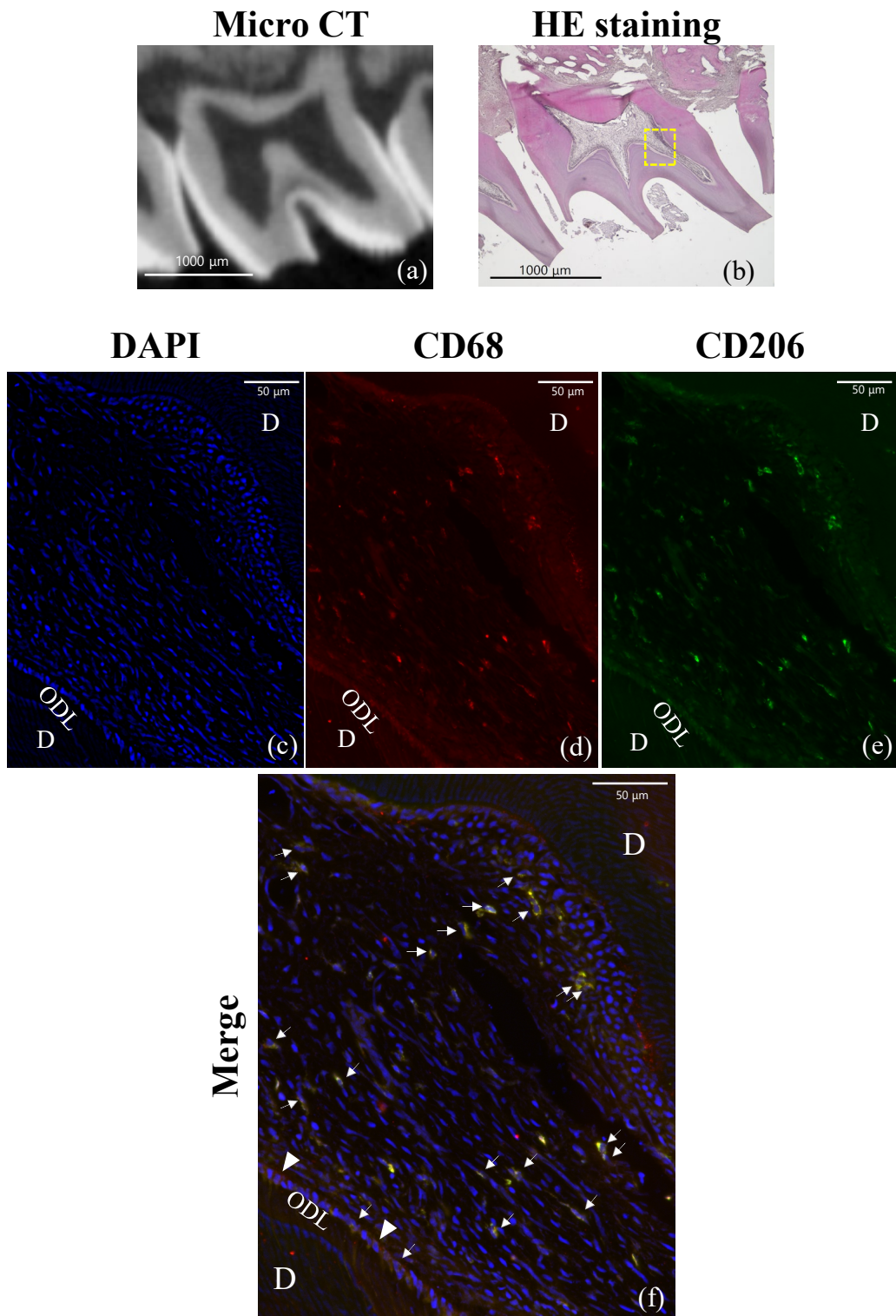


**Figure 5. Macrophage population in the moderate caries group.**

Micro-CT image of a moderate carious tooth in the sagittal plane showing caries invasion to the middle 1/3 of dentin (a). H&E staining reveals that inflammatory cell infiltration was not observed beneath the caries lesion, and odontoblasts maintained a steady distribution (b). Double immunofluorescence staining (c-f) of serial sections from the same specimen show macrophage population in dental pulp under moderate caries progression exhibiting M2 macrophages dominant (f). Arrowhead: CD68(+)/CD206(-) cells. Arrow: CD68(+)/CD206(+) cells. Yellow square: Target area of the fluorescent image. D: dentin.

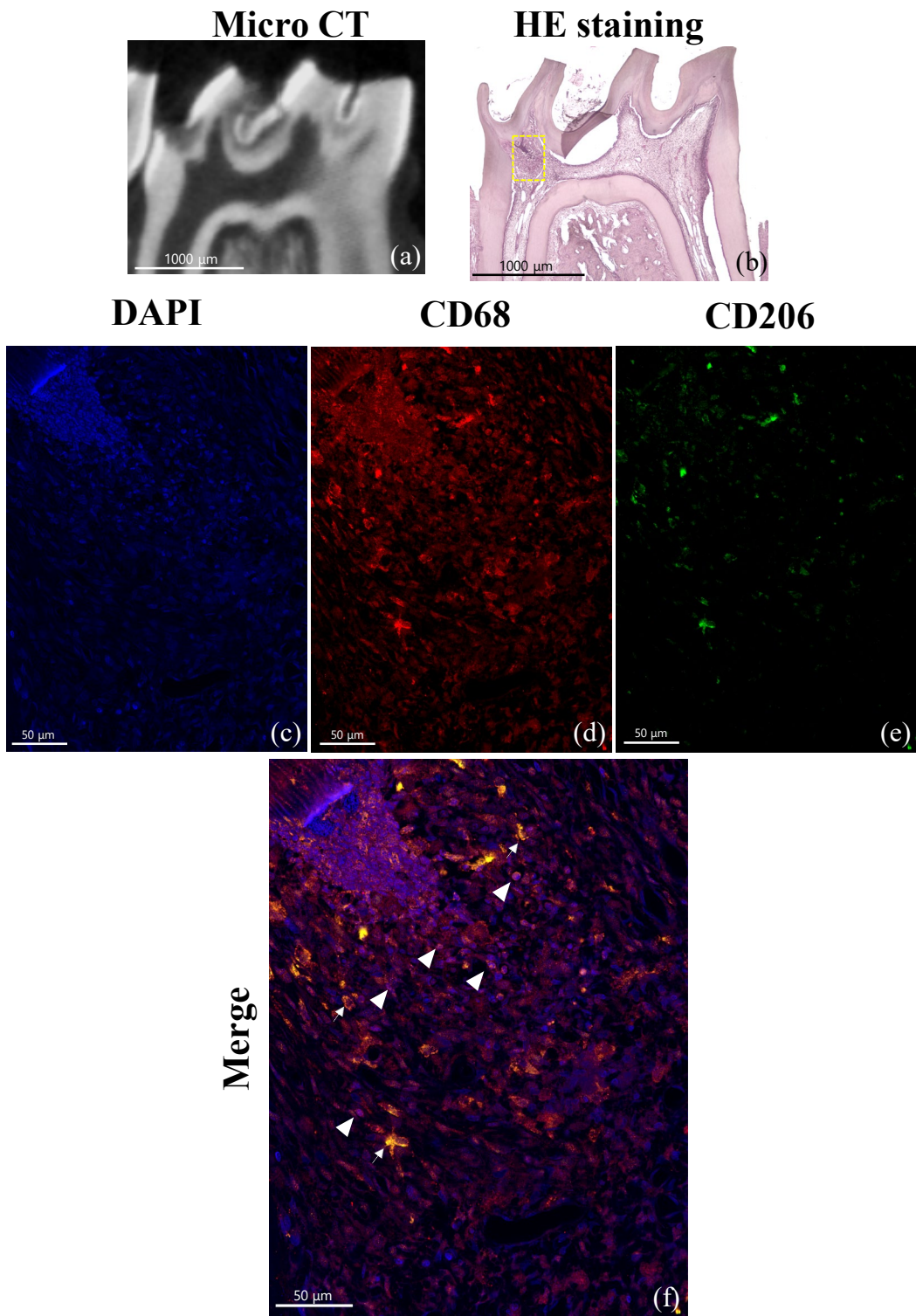


**Figure 6. Macrophage population in the severe caries group without pulp exposure.**

Micro-CT image of the tooth in the sagittal plane indicates caries progressed to the inner 1/3 of dentin (a). H&E staining of serial sections from the same specimen as immunofluorescence staining revealed severe inflammatory cell infiltration beneath the caries lesion (b). Representative images of double immunofluorescence staining in severe caries without pulp exposure (c-f) indicate that M1 macrophages were predominant in severe carious teeth (f). Arrowhead: CD68(+)/CD206(-) cells. Arrow: CD68(+)/CD206+ cells. Yellow square: Target area of the fluorescent image.

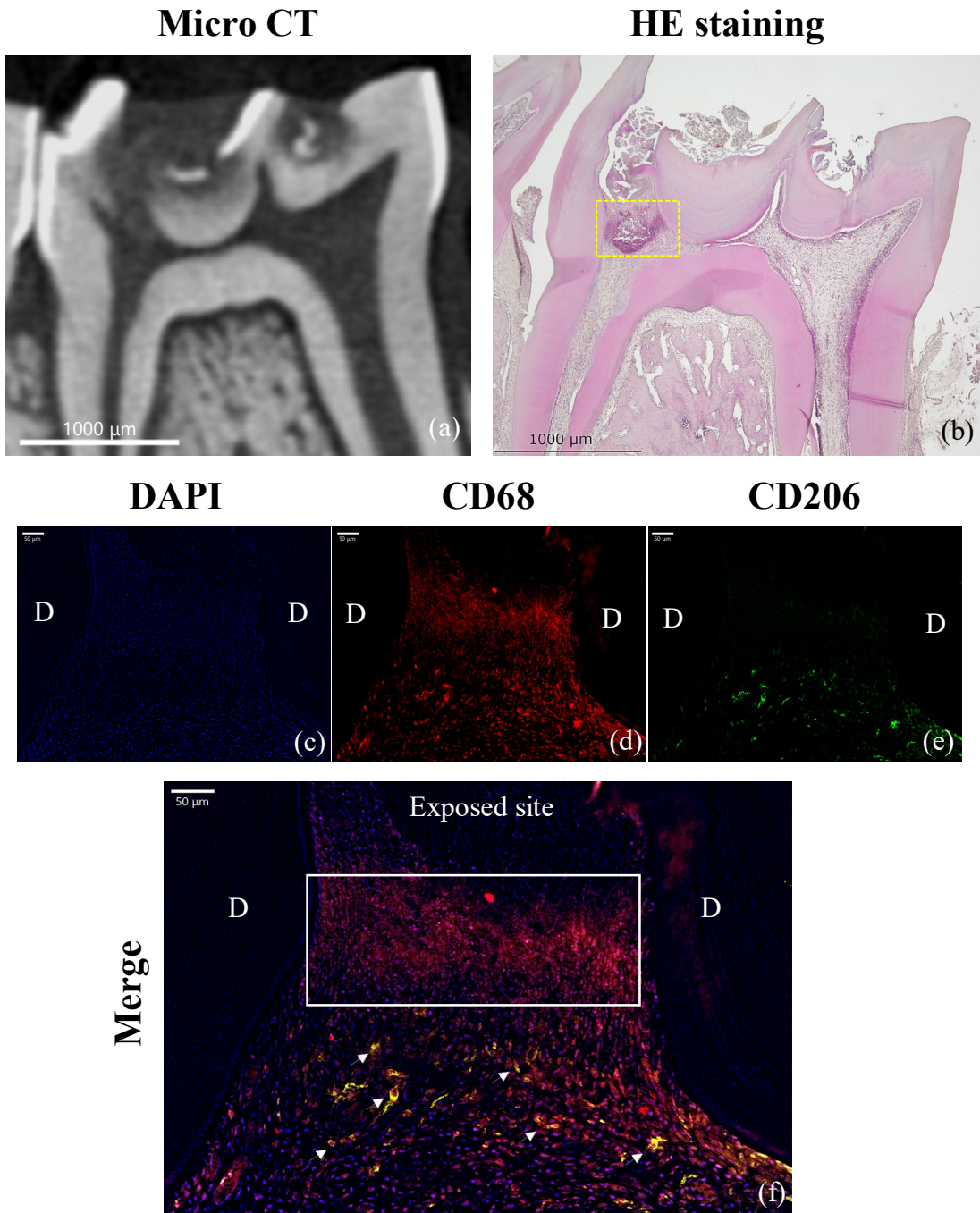


**Figure 7. Macrophage population in the severe caries group with pulp exposure.**

Micro-CT image of the tooth in the sagittal plane indicates that caries proceeded to the severe stage, and pulp exposure occurred in the distal fossa (a). H&E staining of serial sections of the same specimen as immunofluorescence staining revealed severe inflammatory cell infiltration beneath the exposure site (b). Representative images of double immunofluorescence staining in the severe caries with pulp exposure (c-f) show that M2 macrophages were not observed beneath the exposed site (white rectangle), and the pulp exhibited M1 macrophage dominance (f). Arrow: CD68(+)/CD206(+) cell. Yellow square: Image taken at the site of immunofluorescence staining. D: dentin.



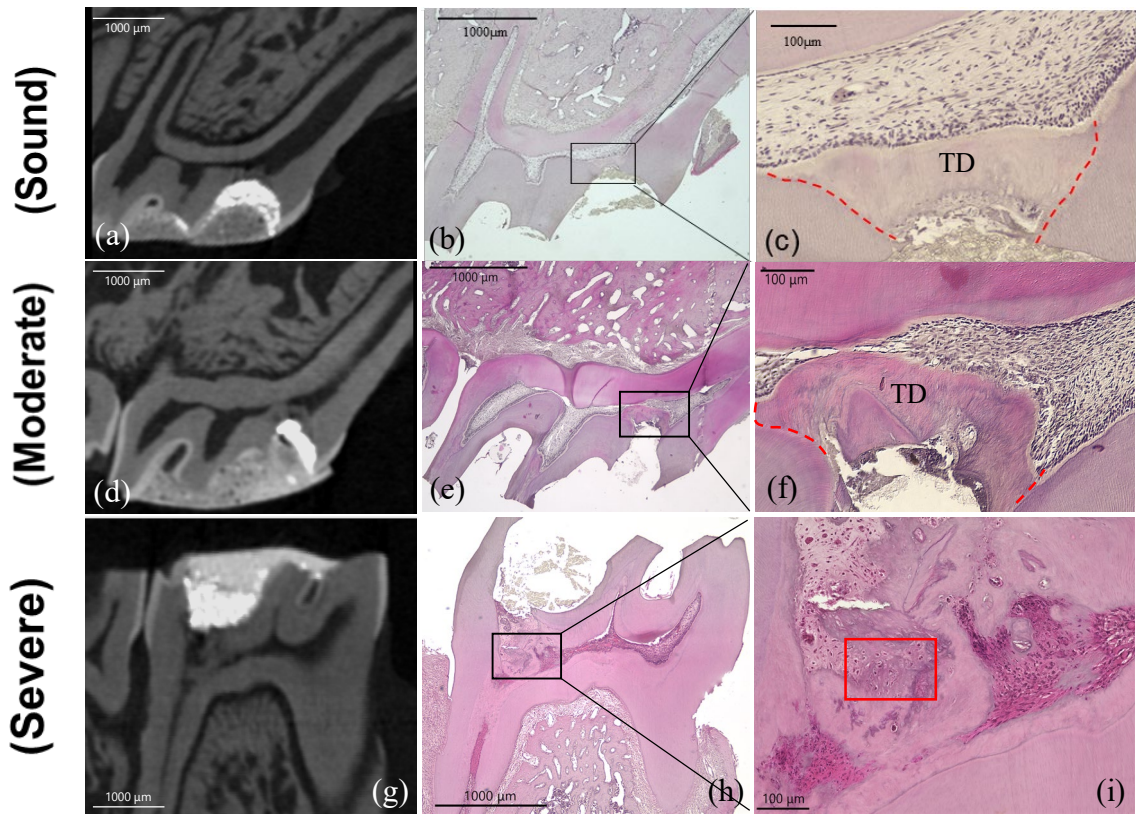


**Figure 8. Histological observation of newly-formed tertiary dentin after pulp capping.** Representative images of micro-CT at 28 days after pulp capping in different carious progression stages (a, d, g). Representative images of H&E staining at low (b, e, h) and high (c, f, i) magnification. Micro-CT images revealed that complete tertiary dentin was formed in the sound (a) and moderate caries (d) groups 28 days post-capping. Incomplete hard tissue was observed in the severe group (g). H&E staining in the sound group shows a well-arranged odontoblast-like cell layer beneath the newly formed dentin bridge in a similar direction to the dentinal tubular structure (c). The moderate group showed an irregular direction of dentinal tubules with disrupted odontoblast-like cell layers (f). Severe inflammation was not relieved in the severe caries group, and calcified tissue with cell infiltration (red rectangle area) was observed (i). Red dashed line: border of newly formed tertiary dentin. TD: tertiary dentin.

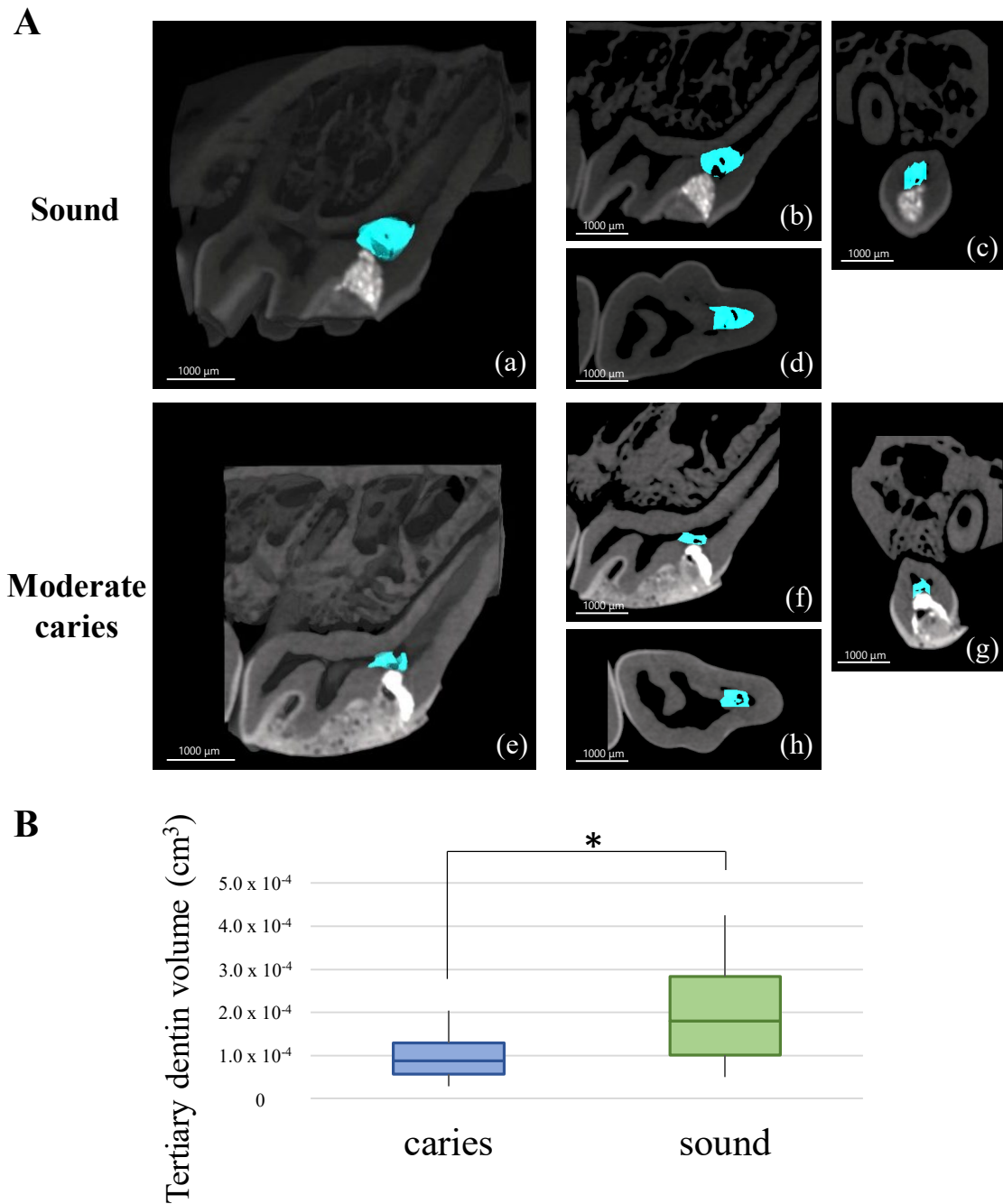


**Figure 9. Comparison of tertiary dentin volume between moderate caries and sound groups.**

A: Representative micro-CT images of tooth structure 28 days after pulp capping. 3D reconstructed images from sound or moderate carious teeth, respectively (a, e). Micro-CT images from three directions: sagittal plane (b, f), coronal plane (c, g), and axial plane (d, h). The tissue selected by blue indicates newly formed tertiary dentin.

B: Quantitative analysis of newly formed tertiary dentin in the sound and caries groups 28 days after pulp capping. A significantly higher volume of tertiary dentin was observed in the sound group. \* indicates significant differences ( $P < 0.05$ , Student's t-test,  $n = 5$ ).

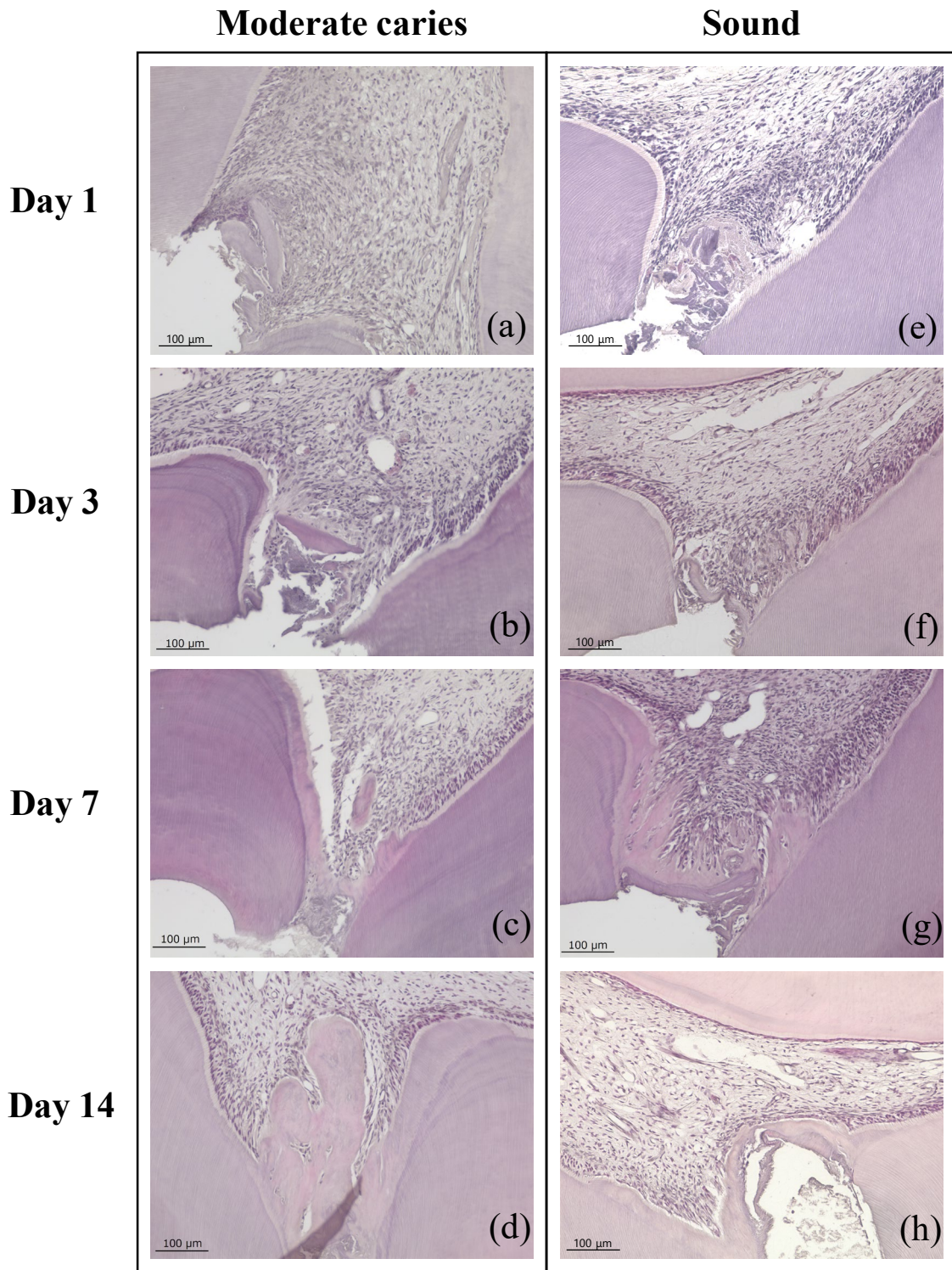


**Figure 10. H&E staining post-capping in moderate caries and sound group.**

The parallel speed of tertiary dentin formation was observed between the moderate caries group (a-d) and the sound group (e-h). Inflammatory cell infiltration was limited beneath the cavity on days 1 and 3 in the sound group (e, f). Cell density was high in the entire pulp area on days 1 and 3 in the moderate caries group (a, b).

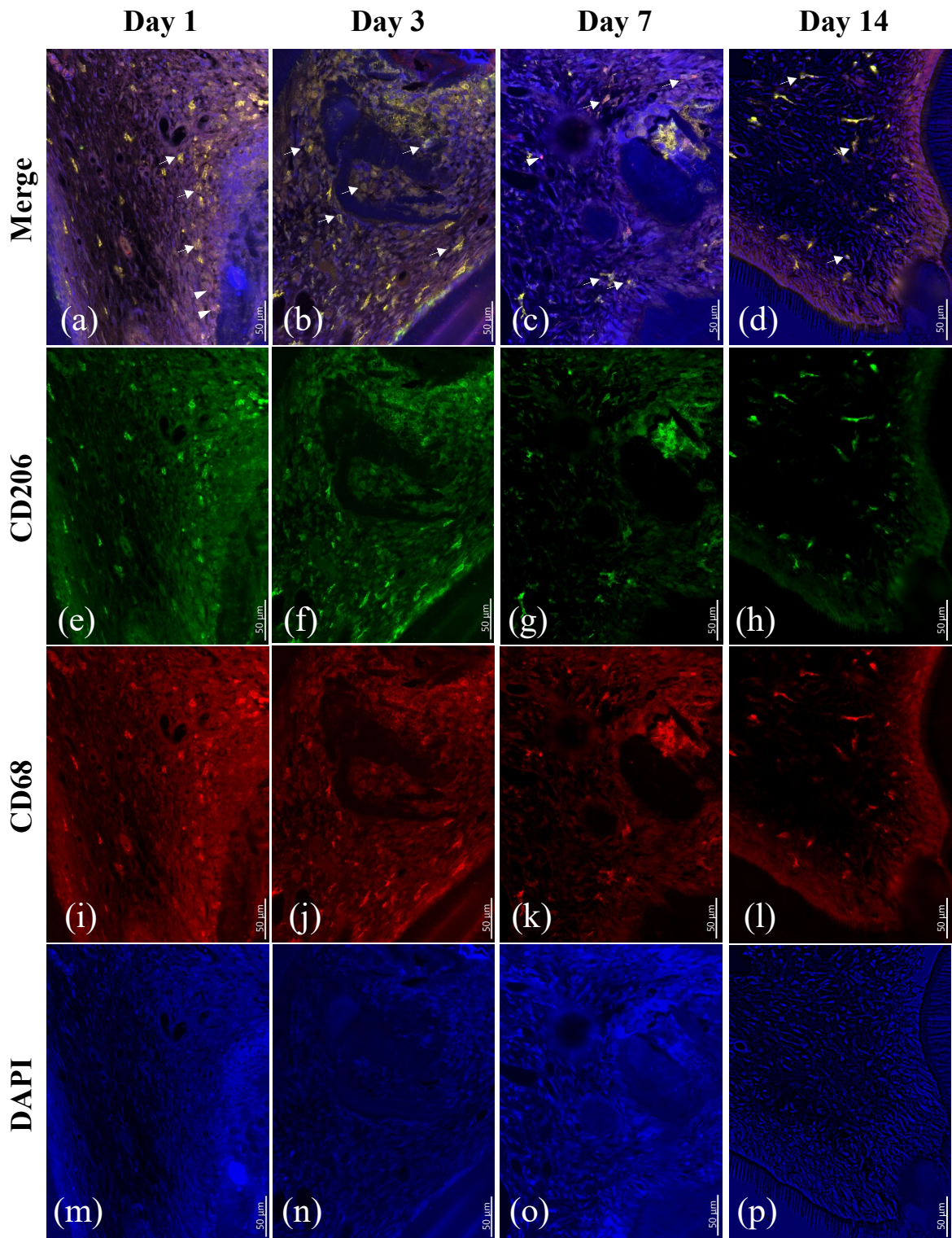


**Figure 11A. Spatiotemporal polarization of macrophage in the moderate caries group at different time points after pulp capping.**

Representative images of double immunofluorescence staining of CD 68 and CD206 on days 1, 3, 7, and 14 after capping in the moderate caries group. M2 macrophages were predominant at each time point post-capping (a-d). Arrowheads: CD68(+)/CD206(-) cells. Arrow: CD68(+)/CD206(+) cells.

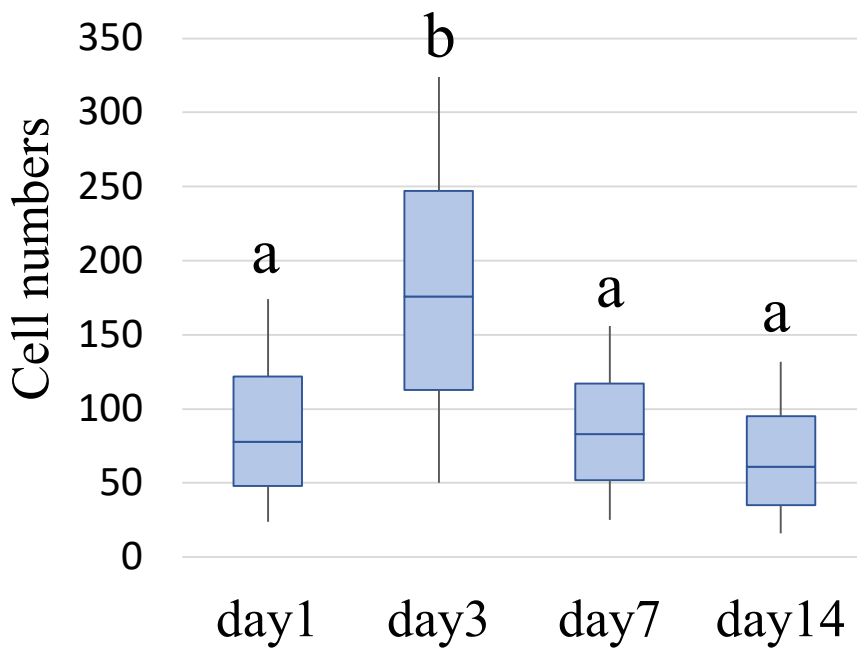


**Figure 11B. Spatiotemporal polarization of macrophage in the moderate caries group at different time points after pulp capping.**

Quantification of double-positive cells in the moderate caries group at each time point post-capping. M2 macrophages showed the maximum population on day 3 and then started to decrease after day 7. Different letters indicate significant differences ( $P < 0.05$ , one-way ANOVA, Tukey's test,  $n = 5$ ).

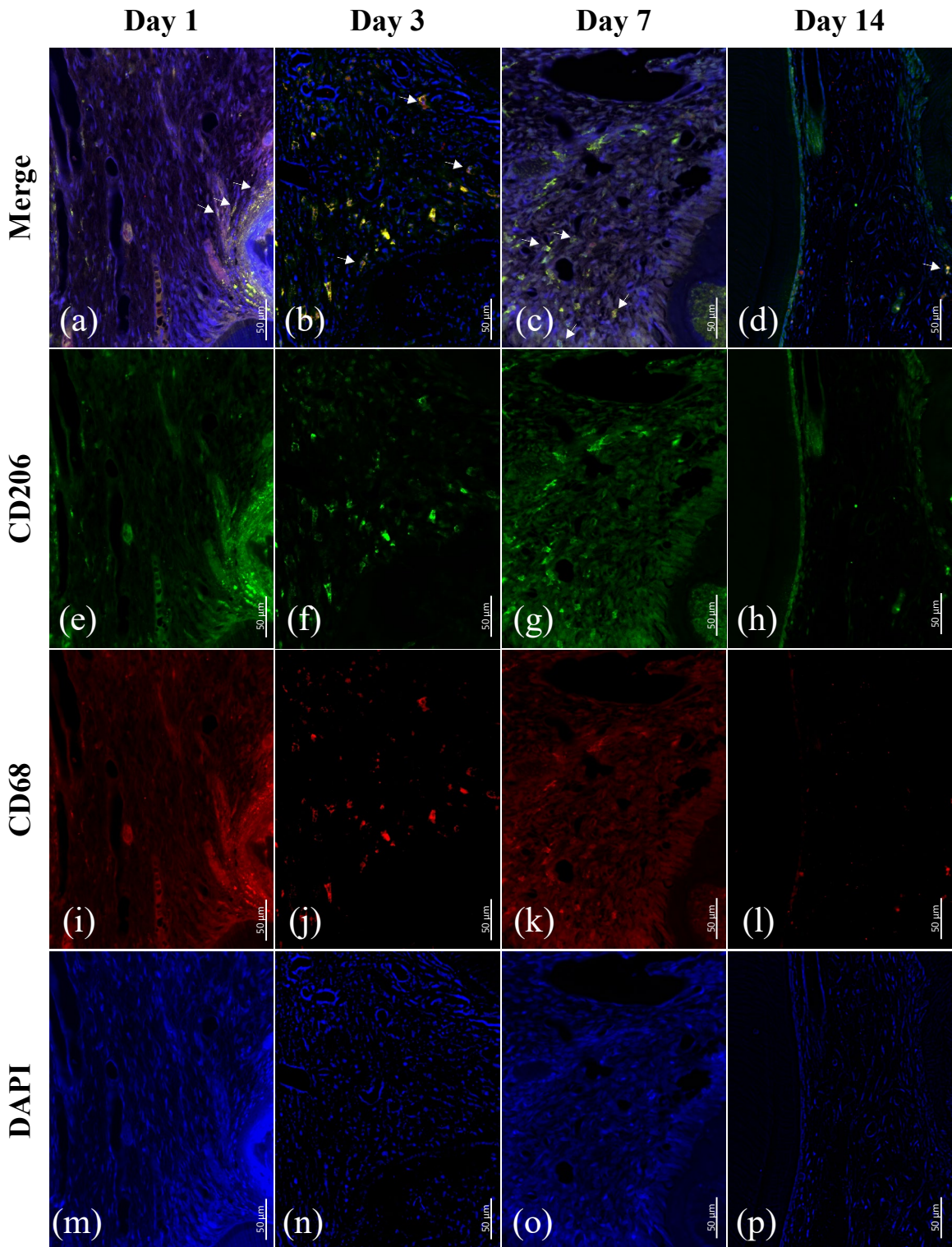


**Figure 12A. Spatiotemporal polarization of macrophage in the sound group at different time points after pulp capping.**

Double immunofluorescence staining of CD68/CD206 after pulp capping in the sound group at different time points. M2 macrophages were also predominant during the wound healing process (a-d). Arrow: CD68(+)/CD206(+) cells.

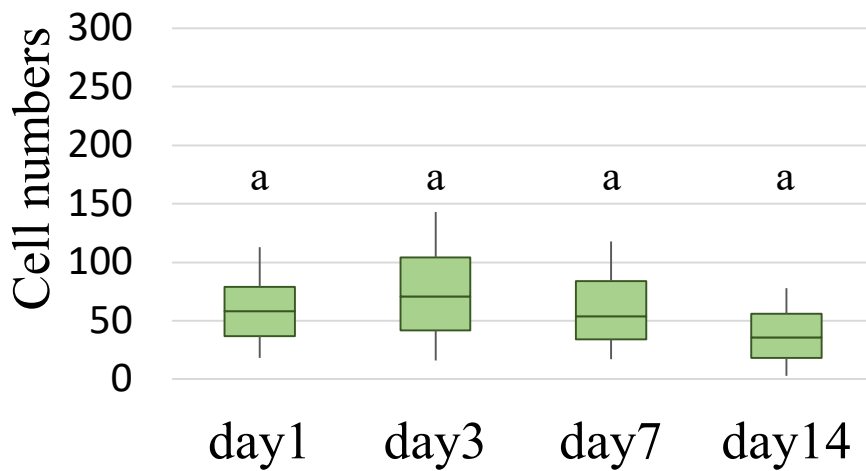


**Figure 12B. Spatiotemporal polarization of macrophage in the sound group at different time points after pulp capping.**

Quantification of double-positive cells in the sound group. No significant changes in the M2 macrophage population were observed throughout the experimental period. The same letters indicate no significant differences ( $P > 0.05$ , one-way ANOVA, Tukey's test,  $n = 5$ ).

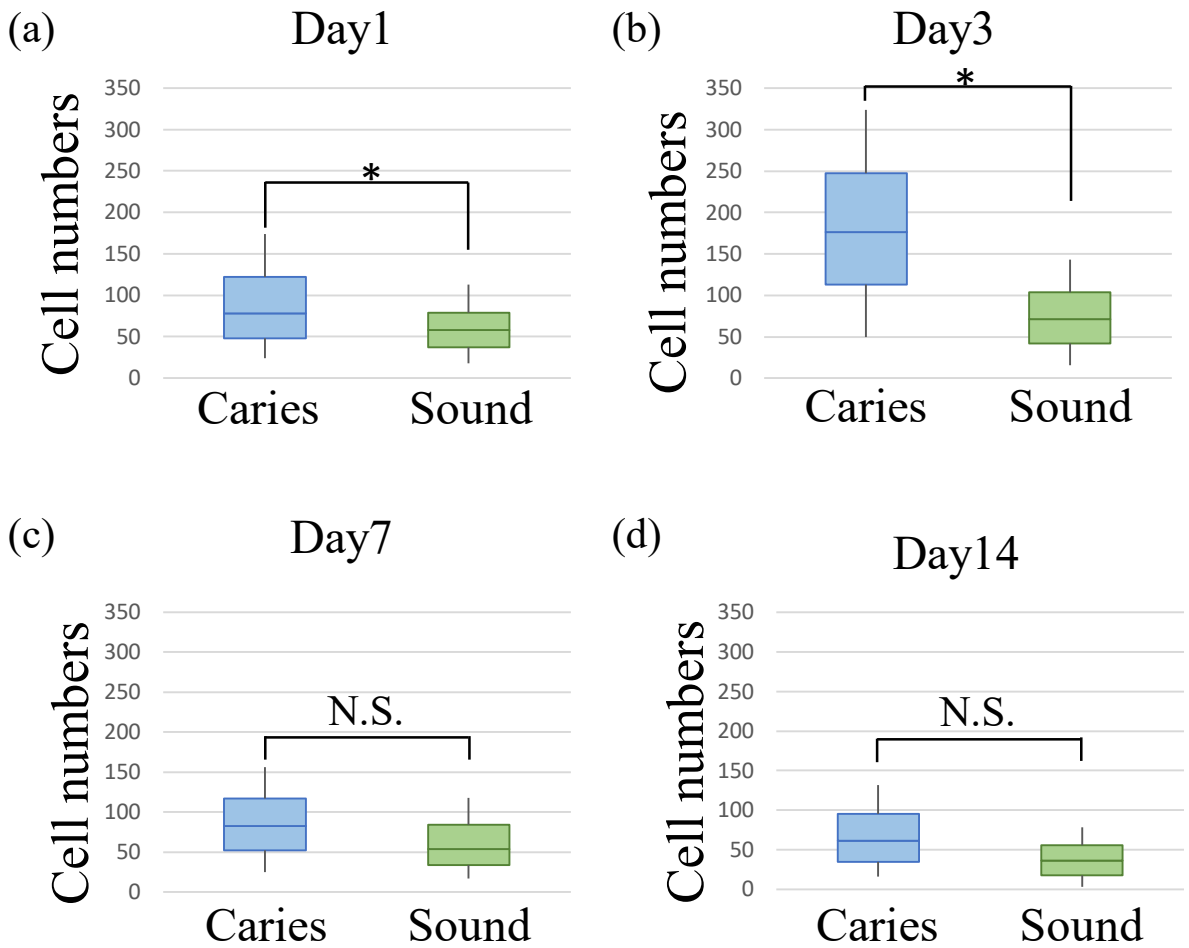


**Figure 13. Comparison of M2 macrophage population at different time points between caries and sound group.**

The number of M2 macrophages in the moderate caries group was higher than that in the sound group on days 1 and 3 (a, b). No significant differences were observed on days 7 and 14 (c, d) (\* $P < 0.05$ , Student's t-test,  $n = 5$ ).



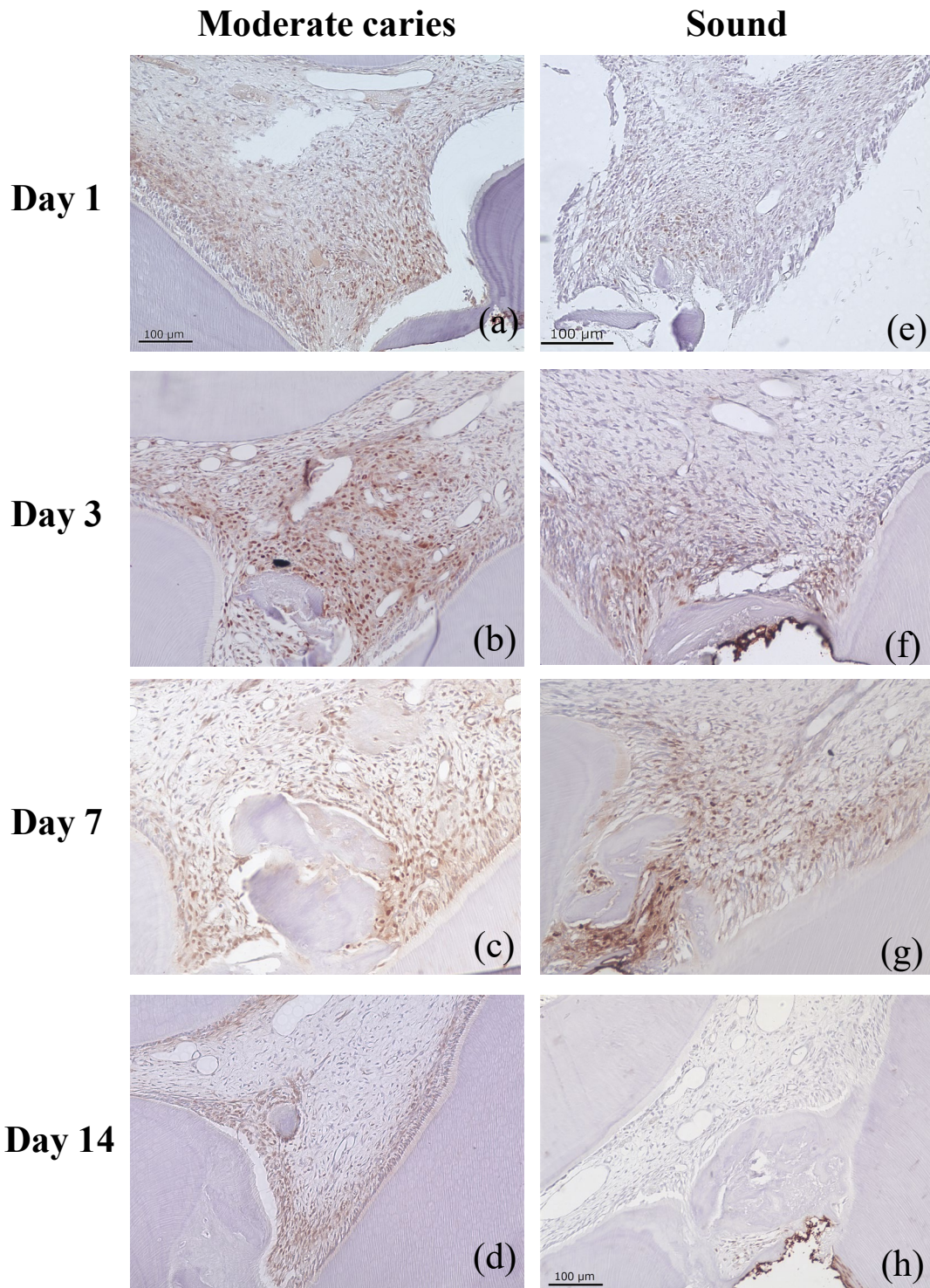


**Figure 14. PCNA expression during the wound healing process post-capping.**

Representative images of immunohistochemical staining for PCNA on days 1, 3, 7, and 14 after pulp capping in the moderate caries (a-d) and sound groups (e-h). PCNA (+) cells were not limited to the pulp horn near the exposure in the caries group on days 1 and 3 (a, b). In the sound group, clustered PCNA (+) cells were observed only in a limited area close to the cavity (e, f, g).

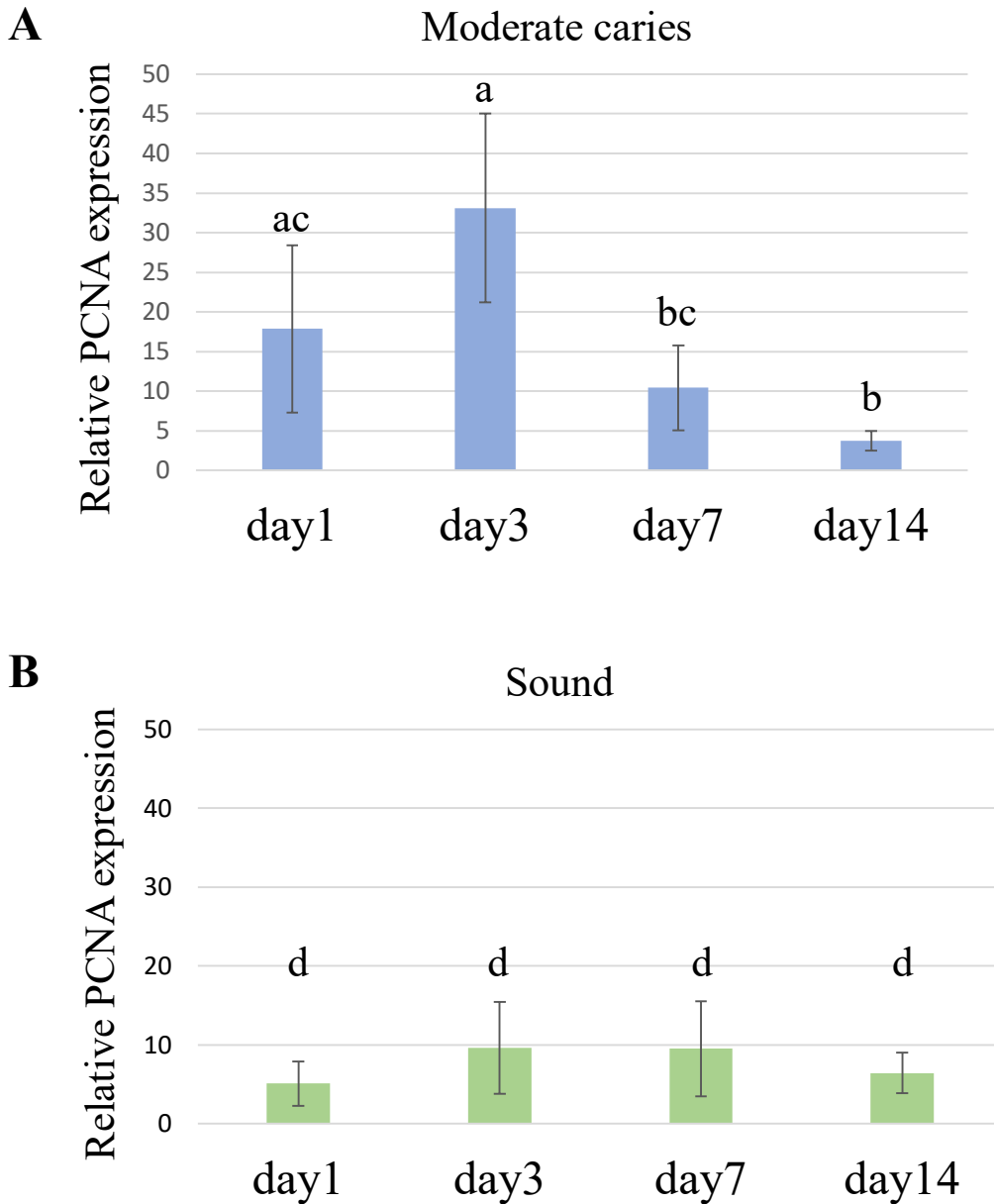


**Figure 15. Relative PCNA expression at different time points.**

A: Quantification of PCNA (+) cell expression in the moderate-caries group. PCNA expression was abundant on day 3 and began to decrease after day 7. Different letters indicate significant differences ( $P < 0.05$ , ANOVA and Tukey's HSD test,  $n = 3$ , error bars indicate standard deviation).

B: PCNA expression in the sound group. No significant upregulation of PCNA was observed. Same letters indicate no significant differences ( $P > 0.05$ , ANOVA and Tukey's HSD test,  $n = 3$ , error bars indicate standard deviation).

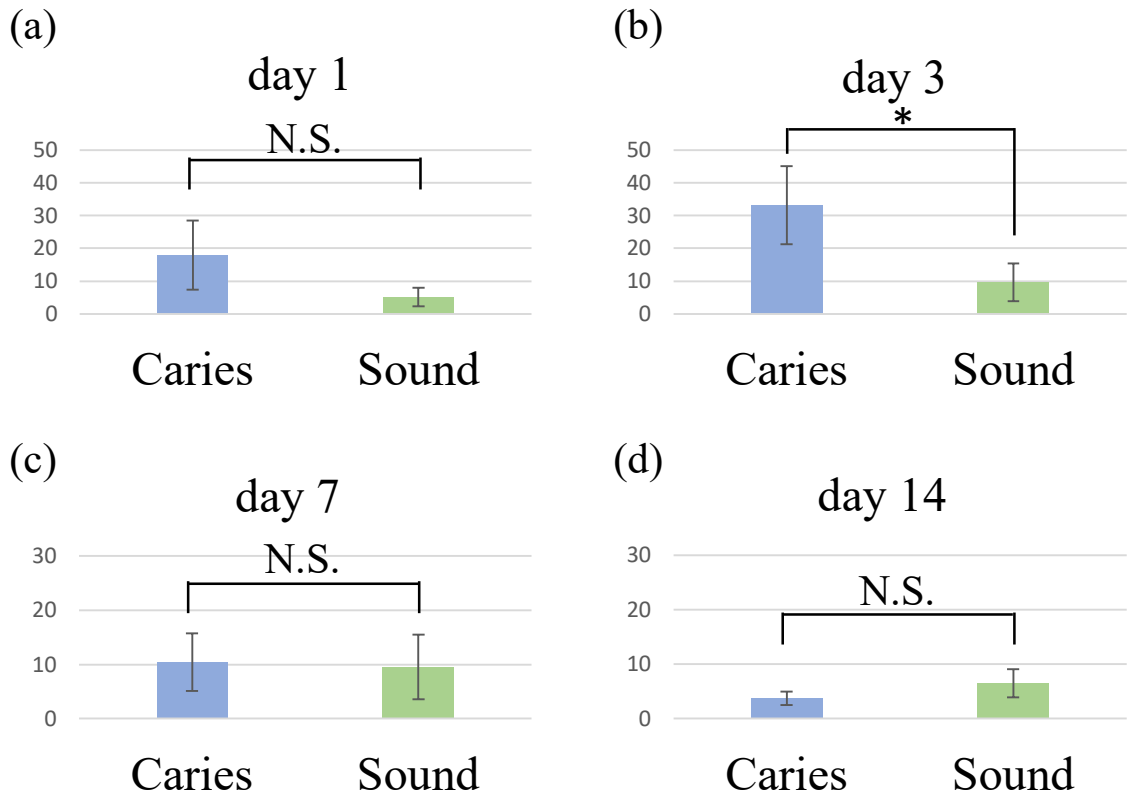


**Figure 16. Comparison of relative PCNA expression between caries and sound groups at different timepoints.**

The caries group showed significantly higher expression of PCNA on day 3 compared to the sound group (b). The other time points showed no significant differences (a, c, and d). \* indicates significant differences ( $P < 0.05$ , Student's t-test,  $n = 3$ , error bars indicate standard deviation).